Fabrication of nanostructured SERS substrates on conductive solid platforms for environmental application

Daniel K. Sarfo, Emad L. Izake, Anthony P. O'Mullane, and Godwin A. Ayoko*

Queensland University of Technology(QUT), School of Chemistry, Physics and Mechanical Engineering, 2 George street, QLD 4001, Australia.

*Corresponding Author

E-mail: g.ayoko@qut.edu.au

Abstract

Due to its high analytical sensitivity and field deplorability, surface enhanced Raman spectroscopy (SERS) has emerged as an analytical tool for detecting environmental toxicants in different matrices. Progress has been made towards development of methods for depositing nanostructures onto solid platforms to design SERS substrates. The properties of the solid platforms used for SERS substrates fabrications such as electrical and heat conductivity, malleability and foldability, have significant influence on the design of the nanostructures and are critical for SERS technique. This review takes a look at recent advances in commonly employed conductive solid materials such as indium tin oxide, carbon fiber, silicon wafers, polyaniline fiber and carbon nanotubes as the supporting platforms for fabricating SERS substrates. It also examines their influence on the fabrication method, the morphology of the nanostructures formed as well as the hot spot density on the resultant novel SERS substrates. Real world applications of these substrates for the detection of environmental toxicants over the past decade have been shown. The review indicates that while significant advances have been made on the use of the conductive properties of these support platforms for SERS substrate fabrication, their subsequent application to detect environmental toxicants have not been fully explored.

Key words: Environmental toxicants, SERS, nanostructures, indium tin oxide (ITO), carbon fibers, silicon wafers, polyaniline fiber (PANI) and carbon nanotubes

1. Introduction

1.1 Surface enhanced Raman spectroscopy (SERS)

Surface enhanced Raman spectroscopy (SERS) is an analytical technique with widespread applications in catalysis (Kim, Barcelo et al. 2012), biomolecule detection (Chan, Liu et al. 2017), environmental monitoring (Bhandari, Walworth et al. 2009) agriculture (Li, Yang et al. 2014, Tang, Dong et al. 2015, Pang, Yang et al. 2016), forensic (Izquierdo-Lorenzo, Alda et al. 2012, Hughes, Izake et al. 2014, Sivanesan, Izake et al. 2015) and food safety (Craig, Franca et al. 2013, Xie, Pu et al. 2017). This is due to its sensitivity, non-destructive nature and the ability to directly screen aqueous samples which are often problematic for other spectroscopic techniques such as infra-red spectroscopy (Wu, Liu et al. 2013). In addition, its multiplexing ability allows for the detection and identification of multiple analytes in a given sample (Culha 2013). Due to the availability of portable and handheld Raman spectrometers, the SERS technique can be easily carried out in the field with minimum sample pre-treatment (Aroca, Alvarez-Puebla et al. 2005, Schmidt, Sowoidnich et al. 2010, Kurouski and Van Duyne 2015).

In SERS, the analyte molecules are adsorbed onto the rough nanostructured metallic surface (usually a noble metal) where the inherently weak Raman scattering from the analyte becomes significantly enhanced (Xie, Qiu et al. 2011, Ding, Yi et al. 2016). Gold and silver are the most widely used metals when fabricating SERS substrates. This is due to the presence of unbound electrons within their electronic structure which supports surface plasmons such as surface plasmon polaritons (SPP) and localised surface plasmons (LSP) (Meyer, Le Ru et al. 2011, Bernardi, Mustafa et al. 2015, Kalachyova, Mares et al. 2016). It is the presence of these surface plasmons which contribute to the enhancement effects observed in SERS. The SPP is a

coherent oscillation of electrons that propagates effectively as a longitudinal wave and occurs between the surfaces of these coinage metals and a dielectric medium (Fig. 1A) (Johns, Yu et al. 2016). The LSP, which is the coherent oscillation of electrons within the vicinity of coinage metal nanostructures (Fig. 1B), can be produced quite easily using Au or Ag nanostructures in the visible to near infra - red region where most Raman measurements are undertaken to avoid fluorescence background (Willets and Van Duyne 2007).

<Insert Fig 1> Fig. 1 Schematic illustration of (A) surface plasmon polariton and (B) localised surface plasmon.

<Insert Fig 2> Fig. 2 Schematic representation of SERS phenomenon for an analyte on Au nanoparticles.

Metals such as Pd, In, Rh and Ru have also been explored in the fabrication of SERS substrates. However, the difficulties associated with their LSP excitation within the visible region of the electromagnetic spectrum, make them less suitable for SERS applications (Ren, Liu et al. 2007).

The enhancement effect of SERS is well-known to originate from a chemical effect, often referred to as a charge transfer mechanism (CT) and an electromagnetic (EM) effect. The chemical effect results from electronic transitions between analyte molecules and the surfaces of the metallic nanostructures onto which the molecules are chemisorbed (Kumar, Shruthi et al. 2007). Electromagnetic enhancement, on the other hand, occurs when the analyte orients itself within the LSP resonance. Upon light incidence, the incoming monochromatic radiation creates a localised electromagnetic field which extends up to ca. 20 nm from the metal surfaces.

The Raman radiation of a molecule within the LSPR (shown as B in Fig. 2) experiences enhancement while those outside the LSPR (A in Fig. 2) do not. A stronger enhancement is experienced when the molecule is trapped within the gap between adjacent metal nanostructures, often referred to as "hotspot", where the LSPR of the nanostructures overlap (C in Fig 2)(Kumar, Shruthi et al. 2007, Hughes, Izake et al. 2014). Resonance enhancement can also occur when the wavelength of the incident light is in resonance with the absorption wavelength of the analyte. A combination of the CT, EM and resonance effects can produce an enhancement to the Raman signal intensity up to 10^{14} (Ko, Chang et al. 2008, Qian and Nie 2008). The Raman signal enhancement observed in SERS is usually quantified using the SERS enhancement factor (EF). EF is mathematically described by equation 1 and it is commonly used to facilitate comparisons between different SERS substrates (Cardinal, Vander Ende et al. 2017).

$$SSEF = (I_{SERS} / I_{RS}) \times (N_{RS} / N_{SERS}) \qquad (1)$$

(I_{SERS} and I_{NRS} are the SERS and conventional Raman scattering intensities, respectively, and N_{SERS} and N_{NRS} are the number of molecules that contribute to the scattering intensity in the SERS and conventional experiments, respectively)

A second metric that is commonly used for assessing the performance of a substrate is the analytical enhancement factor (AEF) (equation (2))(Le Ru, Blackie et al. 2007, Fateixa, Nogueira et al. 2015).

$$AEF = (I_{SERS} / I_{RS}) \times (C_{RS} / C_{SERS}) \qquad (2)$$

(I_{SERS} and I_{NRS} are the SERS and conventional Raman scattering intensities, respectively. C_{RS} is the concentration of the analyte in a test bulk solution and C_{SERS} is the concentration of the analyte adsorbed on the substrate for SERS analysis).

Another metric that is also used to describe the sensitivity of a SERS substrate is the limit of detection (LOD). This metric is used to indicate the minimum concentration of an analyte than can be detected by the substrate using SERS (Cardinal, Vander Ende et al. 2017).

1.2 Fabrication of SERS substrates

Since Raman enhancement is greatly influenced by the choice of SERS substrates, significant advances have been made by many researchers over the past decade on developing a variety of these substrates for SERS measurements. SERS substrates can generally be grouped into two categories: (1) metal nanoparticles (MNP) in suspension and (2) metal nanostructures on surfaces of solid platforms. The use of MNP in suspension for SERS applications come with some advantages among which are the ease of their chemical synthesis, without sophisticated instrumentation, the excellent Raman signal enhancement they can generate and their ability for single molecule detection (Xie, Qiu et al. 2011). However, they are known to suffer from some drawbacks in that, their enhancement factors are often difficult to control. This, in part, is due to the difficulties in producing suspensions containing nanoparticles of uniform/homogeneous sizes. Though this problem has been reduced with recent development of methods that can produce suspensions with homogenous nanoparticle sizes, identifying the precise location of "hotspots" in these suspensions still remains a challenge (Yan, Thubagere et al. 2009). In addition, the aggregation of MNPs are often required for SERS observation (Chen, Li et al. 2014). This requirement is problematic as MNPs aggregation is usually difficult to control. For instance, in some cases the aggregation of MNPs can occur even before SERS spectra acquisition making data collection challenging when using suspension based MNPs. A combination of these issues gives rise to difficulties in signal reproducibility thereby, making reliable and reproducible Raman measurements quite difficult. The attempt to minimise the aforementioned problems has led to the development and utilisation of metal nanostructures on surfaces of solid platforms as SERS substrates. These solid platforms have well-defined

structures that provide stability to the nanostructures they support and improve / create coupling of different SPR modes for better Raman signal enhancement. Since the SERS active nanostructures are fixed on the surfaces of 1D, 2D and 3D solid platforms, the problem of uncontrolled nanoparticle aggregation is essentially eliminated. Furthermore, this approach allows one to control the inter nanoparticle distances which are crucial in the creation of hotspots (Lin, Cui et al. 2009). This is because of the observed electric field enhancement when the inter nanoparticle distances are within the nanometer range. There is an even sharper increase in this electric field enhancement when the adjacent nanoparticles are at a distance <2 nm apart from each other (Zou and Schatz 2005). This was confirmed by Jiang *et al* (Jiang, Bosnick et al. 2003) in their experiment using 60 nm sized Ag nanoparticles separated by 9 nm, 3 nm and 1 nm. From their experiment, enhancement factors increased from 1.5×10^4 to 1.7×10^6 through to 5.5×10^9 for the 9 nm, 3 nm and 1 nm inter nanoparticle distances respectively. As a result, numerous methods have emerged to fashion SERS substrates with nanostructures immobilised on solid platforms such as conductive carbon nanotubes (Zhang, Zhang et al. 2016), polyaniline (PANI) materials (Qian, Liu et al. 2012), silicon wafers (Deng and Juang 2014), carbon fibre cloth (CF) (Zhao, Xu et al. 2014) and indium tin oxide (ITO) (Su, Ma et al. 2011, Bian, Chen et al. 2012). Examples of these methods are lithography (Tan, Agarwal et al. 2007, Coluccio, Das et al. 2009, Yue, Wang et al. 2012), dry reactive ion etching (Whitney, Myers et al. 2004, Hicks, Lyandres et al. 2007) and atomic layer deposition (Liu, Sun et al. 2011) which have been used extensively to build nanopatterned SERS substrates. However, the cost of production and the instrumentation required for their fabrication are relatively expensive and the throughput is usually low (Zhu, Meng et al. 2011). Unlike nonconductive materials, the use of conductive solid support platforms in the design of SERS substrates opens up the possibility of electrophoretic and electrochemical deposition techniques which are relatively more cost-effective routes to fabricating SERS substrates with

homogeneous and reproducible surfaces as well as high density of nanostructures (Lin, Cui et al. 2009). With these methods, applied voltages are either used to immobilise nanoparticles onto conductive solid platforms (by electrophoretic deposition) (Zhu, Zhang et al. 2012, Dushaq, Rasras et al. 2017) or form nanostructures directly on such surfaces (by electrochemical deposition) (Ye, Wang et al. 2010, Wang, Cao et al. 2013) with good mechanical adhesion. In the case of electrochemical deposition, nanostructures can be generated without capping agents. This eliminates the problems of Raman fingerprint interferences which occurs for SERS based applications using chemically synthesised nanoparticles in solution that require capping agents to prevent severe nanoparticle aggregation (Jamil, Izake et al. 2015). In view of the flexibility they present, conductive solid platforms, here referred to as electrodes, have been used extensively as support materials in the fabrication of a variety of SERS substrates.

1.3 Scope of this review

Different kinds of nanostructures have been developed using different fabrications strategies towards the design of SERS substrates and have seen a lot of growth during the past few years (Fig. 3). Considering the wide range of research reporting on the fabrication of SERS substrates using metal nanostructures on solid platforms, it is impossible to review every contribution to this area. Hence, this review is limited to the use of more commonly employed electrode materials such as indium tin oxide (ITO), carbon fibers, silicon wafers, polyaniline fiber (PANI) and carbon nanotubes as the supporting solid platforms for fabricating SERS substrate over the past decade.

<Insert Fig 3> Fig. 3 Number of publications per year from 2009 – 2018 period searched through Web of Science using the keywords "SERS Substrate and fabrication" and "SERS and nanostructures"

The impact that these electrodes have had on SERS substrate development as well as the various methods of fabrication using these electrodes will be discussed. Examples of the application of SERS substrates using these conductive support materials in the analysis of environmental toxicants will also be shown. Although there exist review works reporting on SERS (Ding, You et al. 2017, Panneerselvam, Liu et al. 2018), SERS substrates (Alvarez-Puebla and Liz-Marzan 2012, Ding, Yi et al. 2016, Nguyen, Nguyen et al. 2016) and their applications (McNay, Eustace et al. 2011, Sun, Du et al. 2016, Cardinal, Vander Ende et al. 2017), to the best of our knowledge, the types of solid platforms used as supporting materials (particularly conductive solid platforms) and their impact on the SERS substrates fabricated have not been reviewed.

2.0 Fabricating nanostructures on conductive solid platforms

Though a lot of materials have been used as supporting solid platforms on which nanostructures have been deposited or developed for use as SERS substrates, these materials usually lack electrical conductivity. Hence, it is difficult to introduce fabrication processes that require conductivity of supporting materials into the mix of the variety of available fabrication methods. Below are some conductive solid platforms and how they have been utilised in the design of SERS substrates.

2.1 Indium tin oxide (ITO)

Several methods for the design of SERS substrates using different electrodes have evolved in recent times. ITO has attracted a lot of use as a solid platform for SERS substrate development

because it is relatively inexpensive with properties such as optical transparency, excellent electrical conductivity and good heat tolerance (Setti, Mamián-López et al. 2015). For instance, taking advantage of its electrical conductivity, Zhu *et al* (Zhu, Zhang et al. 2012) deposited a thin film of spherical gold nanoparticles (GNPs) on ITO by electrophoresis (Fig. 4).

<Insert Fig 4 > Fig. 4 FSEM images of GNPs immobilised on ITO by electrophoresis at ≤ 2mins **(a and b),** 8 mins **(c)** and **(d)** High resolution image at 8 mins. Red circles indicate sub-10-nm gaps between neighbouring nanoparticles. From Reference(Zhu, Zhang et al. 2012); Reprinted with permission of Springer.

The ITO served as both the cathode and anode using an inter-electrode distance of 3 mm and an applied voltage of 4.5 V. Random aggregation of the ≈40 to 47 nm sized GNPs sol (prepared by a seed mediated method) was prevented by the use of cetyltrimethylammonium bromide (CTAB) as a capping agent which kept a net positive charge on the GNPs. In addition, this net positive charge ensured mobility of the GNPs under an applied external electric field thereby facilitating deposition onto the ITO electrode. The as prepared SERS substrate detected R6G at a concentration of 10^{-7} M. According to Ye *et al* (Ye, Wang et al. 2010), flowerlike gold nanostructures can be developed directly on an ITO by first coating a polydopamine layer on a bare ITO surface. In this work, the polydopamine layer was made by first dipping ITO in a dopamine solution of Tris-HCl. To obtain the SERS substrate, gold nanostructures (AuNS) were electrodeposited directly onto the polydopamine/ITO electrode via cyclic voltammetry (CV) and chronocoulometry. The dopamine layer not only facilitated rapid gold nucleation but also, the abundant OH groups present in its structure acted as a capping agent which is crucial for both GNP formation and for the control of GNP aggregation. Using R6G as a probe

molecule, a concentration of 10^{-12} M was detected. This work indicated that hierarchical nanostructures with good surface coverage together with exceptional size and shape uniformity can also be achieved using the electrochemical deposition technique. Again, as reported by Bain and co-workers (Bian, Chen et al. 2012), the use of low precursor metal salt concentrations with a complexing agent (such as sodium citrate) can electrochemically generate hierarchical Ag nanostructures (AgNS) with a 28.8% RSD in their size distribution on the surface of an ITO electrode. From their report, a SERS substrate fabricated in this manner can detect R6G at a concentration of 10^{-10} M with a 14.9% RSD in their SERS signal intensity. Another example involving nanostructure development by electrochemical means is the highly dense silver nanoplate arrays synthesised by Liu *et al* (Liu, Cai et al. 2010) in 2010 using a seed-assisted electrochemical growth method (depicted in Fig. 5) on an ITO electrode.

<Insert Fig 5> Fig. 5 A schematic illustration of the preferential nucleation and oriented growth for cross-linking Ag nanoplate arrays: **(a)** random-oriented Ag seeds laying on the ITO substrate, and Ag nuclei are preferentially formed on some <110>-oriented seeds (see arrow's marks); **(b)** oriented growth of the nuclei along the fastest <110> within (111) plane under a low deposition current density; **(c)** cross-linking Ag nanoplate array structure is formed and standing on the substrate vertically. From Reference(Liu, Cai et al. 2010); Reprinted with permission of The Royal Society of Chemistry.

These nanoplates were formed by initially spin coating the ITO with Ag colloidal solution to form Ag seeds. Subsequently, Ag nanoparticles (AgNP) were electrodeposited on the ITO at room temperature using a low current density. Under these conditions, nucleation of Ag nanoplates occurs preferentially on the Ag seeds. Using 4-aminothiophenol, a SERS substrate

with homogeneous SERS signal generation and an EF of $2x10^5$ was achieved from this approach. Elsewhere, Ag micro-spheres consisting of numerous vertically aligned nanosheets, were formed by electrodeposition on an ITO electrode in an aqueous solution of $AgNO_3$ (2 g/L) and citric acid (18 g/L) at a constant current of 0.17 mA for 60 mins (Zhu, Meng et al. 2011). On this solid platform (Fig. 6), adjacent nanosheets had sub-10 nm distances between each other with rough edges. Its usefulness as a SERS substrate originates from both the numerous hot spots found within these sub-10 nm gaps and the presence of the rough edges.

<Insert Fig 6 > Fig. 6 (a–c) SEM images of Ag microhemispheres at different magnification. The inset in (a) is the SEM side view of the microhemispheres. **(d and e)** Cross-sectional SEM views of a microhemisphere. **(f)** The size distribution of the Ag micro-hemispheres in **(a). (g and h)** Differently magnified SEM images of an imperfect Ag microhemisphere. **(i)** TEM image of fan-shaped pieces broken off from an imperfect Ag micro-hemisphere as shown in **(g).** The inset in **(i)** is the SAED pattern from the black circle. **(j)** SERS spectra of 10^{-11} M R6G from five randomly chosen individual micro-hemispheres. From (Zhu, Meng et al. 2011); Reprinted with permission of The Royal Society of Chemistry.

<Insert Fig 7> Fig. 7 A schematic illustration of the seed mediated two step electrochemical approach for deposition of AuNPs on ITO and its utilization for the detection of 4-Mercaptobenzoic acid (p-MBA). From (Wang, Cao et al. 2013); Reprinted with permission of The American Chemical Society.

These nanostructures resulted from nucleation of Ag atoms followed by their fusion into nanoparticle assembled micro-hemispheres. The fused nanoparticles then form layers of rough

nanosheets aided by Oswald ripening effect. A reproducible Raman spectra for 10^{-15} M R6G and an enhancement factor of $7x10^7$ was observed on this SERS substrate. Wang's group has reported a seed mediated two step electrochemical approach to deposit AuNPs on ITO using an electrolyte containing 0.1 mM $HAuCl_4$ and 0.1 M $NaClO_4$ (Fig. 7). (Wang, Cao et al. 2013) This approach generates monodispersed AuNPs on the electrode surface which is vital for Raman signal reproducibility. Their method involved (i) A nucleation step carried out by applying a potential step from +0.89 to -0.80 v (vs SCE) for 10s to ensure nanostructures with high density and monodispersity; and (ii) A growth process using cyclic voltammetry at a potential range from +0.3 to -0.04V (vs SCE). The Au seeds with low particle size distribution (RSD of 24%) produced in the nucleation step, acted as sites for Au preferential growth by the subsequent cyclic voltammetry stage. This led to the generation of a SERS substrate with monodispersed Au nanoparticles. An EF of $1.26x10^6$ was obtained as well as the SERS spectra of 4-mercaptobenzioc acid with a SERS intensity deviation of only 9.2% for 30 spectra (obtained at 1074 cm^{-1}). Another example of a two-step electrochemical approach on an ITO was reported in 2015 where an enhancement factor of 5.9×10^8 was achieved with an LOD of 10^{-11} M for R6G (Wang, Xu et al. 2015). The ITO electrode was coated with reduced graphene oxide–Ag nanoparticle nanocomposite by a two-step chronoamperometric method. This SERS substrate was fabricated using an aqueous solution of diamminosilver ion ($Ag(NH_3)_2]^+$) and reduced graphene oxide with KNO_3 as the supporting electrolyte. The advantage of graphene oxide in this approach is its high molecular absorption capacity as well as being electron rich which greatly enhanced the charge transfer effect in SERS measurements. Despite the many reports on ITO as a support platform for SERS substrates, the conductive layer can easily be damaged with little mechanical contact. In addition, moulding them into different shapes and designs poses a challenge as special tools are required for this because of their brittle nature. Table 1 below is a list of some SERS applications using ITO-based SERS substrates.

<Insert Table 1> Table 1: SERS applications on environmental toxicants using ITO-based SERS substrates

2.2 Polyaniline (PANI)

Polyaniline (PANI) is an inherently conductive polymer because of the conjugated π electron system present in its structure. It has been utilised as a solid supporting material in the design of different SERS substrates due to its light weight, good electrical conductivity, low cost, ease of synthesis and stability (Zhang, Ji et al. 2007). Unlike ITO, it can easily be cut into different sizes and shapes due to its flexibility without the need for special tools or equipment (Bhadra, Khastgir et al. 2009, Mostafaei and Zolriasatein 2012).

<Insert Fig 8> Fig.8 SEM images of **(a)** Au nanoparticles grown on a PANI membrane (doped by citric acid) by immersing the PANI membrane in 10 mM $AuCl_3$ aqueous solution for 10 s, and the Ag nanostructures produced by immersing the Au nanolayer-supported PANI membrane in 50 mM $AgNO_3$ aqueous solution for **(b)** 10 s**, (c)** 30 s, **(d)** 1 min, **(e)** 10 min, and **(f)** 60 min. The scale bar is 500 nm. From (Xu, Mack et al. 2010); Reprinted with permission of The American Chemical Society.

The abundance of reactive NH- groups in its polymer chain and the ability of these groups to act as reducing agents promotes the formation and deposition of MNPs directly on the surfaces of PANI making it a good candidate as a support material for SERS substrate development. These properties were explored by Xu and co-workers (Xu, Mack et al. 2010) to fabricate a SERS substrate via the direct formation of homogeneous 3D Ag nanostructures on an Au coated PANI membrane. In the fabrication process, the Au coated PANI membrane, which

was obtained by immersing citric acid doped PANI in an $AuCl_3$ aqueous solution, was subsequently dipped into an aqueous solution of $AgNO_3$. This led to the formation of a continuous Ag thin film on the Au surface followed by the growth of Ag nanospheres. The as prepared SERS substrate (Fig. 8) produced a SERS response with an average enhancement factor of 10^6-10^7 using mercaptobenzioc acid. Li *et al* (Li, Xiong et al. 2014) also proposed a dual acid doping technique for the fabrication of SERS active substrates from PANI. In their work, they used ascorbic acid as a reducing agent together with succinic acid which controlled the morphology of the Ag nanoparticles formed on the surface of PANI. This technique greatly enhanced the growth rate of AgNPs and produced Ag nanostructures with morphologies that favour SERS. R6G was detected at a concentration of 10^{-10} M on this SERS substrate.

According to He *et al* (He, Han et al. 2012), homogenous Ag nanostructures can also be generated on undoped PANI within a minute to yield a SERS substrate. This can be achieved by introducing hydrazine and an organic acid in the fabrication process. Hydrazine converts the emaraldine base form of PANI into the leucoemaraldine form which is thermodynamically favourable for rapid reduction of Ag^+ ions. The organic acid, on the other hand, directs the growth of Ag nanostructures ensuring homogeneity and wide coverage on the surfaces of PANI. When salicylic acid, citric acid, succinic acid and lactic acid were tested by He *et al* (He, Han et al. 2012) for comparison purposes, succinic and lactic acid yielded the best SERS performance (Fig. 9). After the SERS substrate was tested with 4-mercaptobenzioc acid, a concentration of 10^{-8} M was detected. Likewise, Yan *et al* (Yan, Han et al. 2012) deposited Ag nanostructures on doped PANI from $AgNO_3$ in succinic acid, camphorsulphonic acid and lactic acid. Again, the lactic and succinic acid solution gave the best surface coverage and homogeneity with good SERS performance (Fig. 10). Here, PANI was first doped with the acid which was used to prepare the $AgNO_3$ solution (i.e. either succinic acid, lactic acid or camphorsulfonic acid). This doping process was very crucial for the homogeneity and full

coverage of nanostructures over the PANI's surface. This is because the nucleation of Ag seeds on PANI is greatly elevated by surface wettability provided by the doping process. The wettability phenomenon will be less (without first doping the PANI) if only the acid used in the $AgNO_3$ solution preparation was available for use.

<Insert Fig 9> Fig. 9 SEM images of Ag nanostructures produced on hydrazine treated PANI films at a reaction time of 30 s **(a)**, 1 min **(b)**, 2 min **(c)** and 5 min **(d)**, with lactic acid present; and 30 s **(e)**, 1 min **(f)**, 2 min **(g)** and 5 min **(h),** with succinic acid present in the $AgNO_3$ solution. Scale bar: 3 mm. From (He, Han et al. 2012); Reprinted with permission of The Royal Society of Chemistry.

<Insert Fig 10> Fig. 10SEM images of Ag nanostructures produced on the camphorsulfonic-acid-doped PANI membranes, with **(a, b)** succinic acid, **(c, d)** lactic acid, and **(e, f)** camphorsulfonic acid present in the AgNO3 solution. From (Yan, Han et al. 2012); Reprinted with permission of The American Chemical Society.

A SERS signal response was realized, at a concentration of 10^{-12} M for 4-mercaptobenzioc acid, when the doped PANI membranes were used with $AgNO_3$ solution containing succinic acid in the SERS substrate fabrication process. Mondal *et al* (Mondal, Rana et al. 2015) also fabricated a recyclable SERS substrate using polyaniline fibers doped with benzene tetracarboxylic acid. The doped material acted as a reducing agent, template and stabilizer. They were able to detect 4-mercaptobenzoic acid and R6G by SERS in the nanomolar concentration range.

One drawback associated with the use of PANI is the aniline group in this material. This group is Raman active and hence possess background interference challenges, particularly, when the

fabrication method is not tuned to properly cover the entire polyaniline surface. Though PANI is electrically conductive, the use of applied voltages for the development of highly dense nanostructures on their surfaces towards SERS substrate design is still an underdeveloped area. Besides, in as much as PANI has been used as a solid support material on which MNPs have been deposited towards the fabrication of SERS substrates, to the best of our knowledge, very little can be found in literature on the use of such SERS substrates for real life applications. However, solution based Ag@PANI and Au@PANI have been used for the detection of Hg(II) ions at concentrations of 1 pM and 10 pM respectively (Wang, Shen et al. 2011, Wang, Shen et al. 2013). The detection mechanism was based on nanoparticle aggregation triggered by the attachment of Hg (II) ions to the nitrogen atoms of PANI.

2.3 Carbon based solid platforms

Carbon nanotubes (CNTs) which are elongated fullerenes or rolled graphene cylinders are known to be potential surface plasmon enhancers and hence have attracted applications in the fabrication of SERS substrates (Sun, Liu et al. 2010, Dresselhaus and Terrones 2013). Due to their high strength, good chemical stability, electrical conductivity and the fact that they are nanoporous in nature, they can be used as templates for the direct electrochemical deposition of nanostructures on their surfaces with excellent control over nanoparticle size and density (Chen, Young et al. 2007, Dresselhaus and Terrones 2013). Carbon fibers (CFs) have also been used in SERS substrate development due to their flexibility, high conductivity, good corrosion resistance and large surface area. With the emergence of CFs, the design of easily foldable and portable SERS substrates that can be fashioned into different shapes to suit different applications is achievable (Zhao, Xu et al. 2014). Unlike PANI and other organic based support platforms, which may pose background interference problems due to the presence of relatively high polarizable molecules with extended π–π systems and electron-rich atoms, clean CNTs and CFs have the advantage of producing insignificant background signal interferences

(Halvorson and Vikesland 2010). By virtue of the positive features of CNTs, Beqa *et al* (Beqa, Singh et al. 2011) designed a SERS substrate by decorating an aminothiophenol (ATP) functionalized CNT with popcorn and rod shaped Au nanostructures separately and evaluated their SERS performance. The popcorn shaped nanostructures yielded the best results due to the existence of sharp edges and corners on the nanostructures. Whilst the central sphere of the popcorn shaped Au nanostructures acted as electron reservoirs, their tips contributed positively to the field enhancement by concentrating the electric field at their apexes. A 10^{-9} M R6G concentration was detected and a SERS enhancement factor of 8.9×10^{11} was observed on this SERS substrate. Likewise, Jiang, Zhang and collaborators (Jiang, Zhang et al. 2011) developed a nest-shaped CNT, incorporated it in a silicon nanoporous pillar array and coated it with an Au film which possessed nanoscale surface roughness. The nest-shaped CNT provided a large surface area for efficient target molecule adsorption. This property, combined with the nanoscale surface roughness of Au, lead to the SERS detection of R6G at a concentration of 10^{-8} M.

<Insert Fig 11> Fig. 11 FE-SEM images of gold nanoparticles patterned onto SWCNT films by electrochemical deposition. The deposited charges for **(A), (B),** and **(C)** were 1 mC, 10 mC, and 30 mC, respectively. The scale bars in the left, middle and right columns are 100 μm, 10 μm and 1 μm, respectively. From (Bui, Lee et al. 2009); Reprinted with permission of The Royal Society of Chemistry.

Bui and co-workers (Bui, Lee et al. 2009) also demonstrated the possibility of producing patterned Au nanostructures on carbon nanotube solid platforms (Fig. 11). The Au deposition was done electrochemically from a 1 mM aqueous solution of $HAuCl_4$ using chronocoulometry

at a set voltage of 0.6 V vs Ag/AgCl. A SERS enhancement factor of 3.0 x 10^4 was obtained using 10 mg/ mL $K_3[Fe(CN)_6]$. Zhao *et al* (Zhao, Xu et al. 2014) have reported that, R6G at a concentration of 10^{-14} M with good SERS signal reproducibility can be realized when Ag nanoparticles are deposited on CFs using an electroless plating method whereby Tollen's reagent was used as the silver source and glucose as the reducing agent. Duy *et al* (Duy, Yen et al. 2016) have also fabricated a SERS and an electrochemical based substrate by electrochemically creating Au nanodendrites on CFs from a solution containing $HAuCl_4$, H_2SO_4, KI and NH_4Cl. In this work, preferential nanodendrite formation was made possible by the introduction of iodide which inhibited nanoparticle aggregation. 2-naphthalenethiol was detected at 1 nM by SERS (with a good substrate-to-substrate reproducibility with an RSD of 8.5% and an EF of $4x10^6$) and 0.09 ppb Hg(II) by stripping voltammetry.

Noble metal-semiconductor nanocomposites such as Ag-decorated $NiCo_2O_4$ (Wang, Zhou et al. 2016), Ag-decorated TiO_2 (Li, Hu et al. 2012, Xie, Jin et al. 2014), Ag-decorated ZnO (Deng, Fan et al. 2009) and Au-decorated SnO_2 (Rodriguez-Fernandez, Langer et al. 2015) have also been incorporated in the fabrication of SERS substrates. This is because of their ability to enhance the CT mechanism of SERS via electron promotion from the semiconductor to the MNPs. This increases the available number of electrons needed for CT between adsorbed molecules and the MNPs (Yang, Ruan et al. 2008, Deng, Fan et al. 2009). Atomic layer deposition (Wang, Meng et al. 2014), vapor-liquid-solid (VLS) growth mechanism (Huang, Chen et al. 2015), hydrothermal method (Bian, Chen et al. 2012) and electrodeposition have therefore been used to graft these semiconductors onto CFs to ensure greater SERS activity. ZnO has attracted much attention because of its superior refractive index that promotes strong light confinement which is essential for SERS activity (Yang, Ruan et al. 2008, Deng, Fan et al. 2009). With respect to this phenomenon, Wang *et al* (Wang, Meng et al. 2014) developed a SERS substrate by grafting ZnO mesoporous nanosheets (ZnO-NS) on CFs using atomic layer

deposition method (Fig. 12). This method involved immersion of the ZnO-seeded CFs in a precursor solution(zinc nitrate and urea) and then placing it in an oven (at 90 °C) for subsequent deposition using $Zn_4(CO_3)(OH)_6 \cdot H_2O$. The formed ZnO-NS were subsequently decorated with AgNPs using an ion-sputtering technique. Good signal reproducibility was achieved from this SERS substrate and was used to detect R6G at a concentration of 10^{-10} M. Table 2 below lists some SERS applications using carbon based SERS substrates.

<Insert Fig 12> Fig. 12 (A) ZnO-mesoporous-NSs grafted on CFs **(a)** Top-view SEM image. The lower-left inset is an optical photo of a piece of ZnO-mesoporous-NSs@CFC. **(b)** Magnified SEM observation on two adjacent CFs grafted with ZnO-mesoporous-NSs. **(c)** Close-up SEM view of a few ZnO-mesoporous-NSs. **(d)** TEM image of a single ZnO-mesoporous-NS and its corresponding selected area electron diffraction pattern; (B) SEM images of Ag-NP decorated on ZnO-mesoporous-NSs with (a) 20 s, (b) 60 s, (c) 120 s and (d) 180 s Ag sputtering time. From (Wang, Meng et al. 2014); Reprinted with permission of The Royal Society of Chemistry.

<Insert Table 2> Table 2: SERS applications on environmental toxicants using carbon-based SERS substrates

2.4 Silicon wafers

Silicon wafers are another type of electrode that have seen a lot of use in SERS substrate fabrication due to silicon's excellent electronic and mechanical properties, biocompatibility and surface tailorability (Jiang, Jiang et al. 2012). Porous silicon wafers have penetrable structures with large surface area which allow for the formation of nanoparticles inside their

holes to yield highly sensitive SERS substrates (Chursanova, Germash et al. 2010). Moreover, coinage MNPs can be grown *in situ* on the surfaces of silicon wafers without the use of templates or surfactants. In addition, the random aggregation of free metal NPs can also be controlled by this synthesis approach resulting in SERS substrates with excellent reproducibility (He, Fan et al. 2010, Peng, Su et al. 2014). Shao *et al* (Shao, Que et al. 2012) demonstrated this by depositing Cu nanoparticles, which are thought to have limited SERS effect, *in situ* on a Si wafer giving rise to an EF of $2.29x10^7$ and a relative standard deviation of < 20% using R6G. They reported that, the said method can be used to prevent nanoparticle aggregation or growth that can result from laser irradiation during SERS detection. This *in situ* growth of metal nanoparticles on the surfaces of Si wafers can be achieved by simply immersing the porous silicon wafer into solutions containing the coinage metal ion of interest. The metal ions, are then reduced via the presence of Si-H bonds which can be introduced on the wafer's surface by a galvanic displacement reaction method (GDR). Giorgis *et al* (Giorgis, Descrovi et al. 2008), Panarin *et al* (Panarin, Terekhov et al. 2010) and Chursanova *et al* (Chursanova, Germash et al. 2010) have all successfully fabricated SERS substrates by immersing porous Si wafer into an $AgNO_3$ solutions after forming the Si-H bonds on the wafer's surface by the GDR method. According to the Jiang's groups (Jiang, Jiang et al. 2012), this method involves a hydrogen fluoride (HF) etching technique, which can produce a highly sensitive and reproducible SERS active substrate that is capable of yielding SERS enhancement factors of about $8.8x10^6$ and a RSD of 12.4%. As this process involves chemical etching, it is debatable whether this truly is a galvanic displacement reaction. However, the cost-effective nature, simplicity and facile feature of this method, along with its ability to generate nanoparticles of high purity with good nanoparticle adhesion to surfaces of Si wafers, motivated the Rajkumar group (Rajkumar, Jayram et al. 2016) to fabricate a SERS substrate using this synthetic route. In their work, a discontinuous film of hierarchical Ag nanostructures

was formed on Si wafers which resulted in a SERS substrate that could detect R6G at a concentration of 10^{-16} M by SERS. Unlike glassy materials, like ITOs, which are relatively fragile, nanoholes acting as sites for nanoparticle deposition can be mechanically patterned in a compact Si wafer and subsequently used as a supporting material for SERS substrate fabrication without any breakage or deformity. For instance, back in 2009, Alexander and co-workers created patterned nanohole arrays with 120 nm by 100 nm hole depth (WxH) and a center-to-center spacing of 350 nm using a soft lithographic technique, known as Pattern Replication in Nonwetting Templates (PRINT) (Alexander, Hampton et al. 2009). Here, nanoclusters comprising of two 60 nm sized gold nanospheres were deposited in these nanoholes by immersing the patterned Si wafer in an aqueous solution of colloidal gold nanoparticles (Fig. 13). Before the deposition process, the Si wafers were made hydrophilic through plasma etching. An EF range of 10^8–10^9 was recorded using thiophenol.

<Insert Fig 13> Fig. 13 (a) Scanning electron micrograph of an array of nanoholes patterned into a Si wafer after Cr deposition, removal of PLGA posts, and reactive ion etching. **(b)** Aspect of whole wafer patterned with nanoholes. From (Alexander, Hampton et al. 2009); Reprinted with permission of Wiley online library.

Fang *et al* (Fang, Agarwal et al. 2008) have also demonstrated that, ordered arrays of silicon nanostructures can be fabricated just from the Si wafer itself by UV photolithography. According to the authors, these nanostructured arrays can be coated with a 30 nm thick layer of Ag followed by an Au layer (of 15 nm thickness) using an E beam evaporation system. The 15 nm Au layer was used as a protective covering for the unstable Ag layer and to prevent peeling during sample incubation periods. Though lithographic techniques generate patterned

surfaces which are essential for reproducibility in SERS, it is limited by the difficulties that comes with fabricating arrays that have interparticle separation less than 10 nm (Yan, Thubagere et al. 2009). For this reason, this technique produces SERS substrates with nanoparticle separations limited to 10 nm - 20 nm which is larger than that theoretically predicted for giant electric field enhancements (Su, Wei et al. 2003, Atay, Song et al. 2004). SiO_2 and semiconductor materials such as ZnO can be grown into nanorods and nanopillars on Si wafers and used as platforms for designing 3D nanostructured SERS substrates of similar patterned surfaces. Hau *et al* (Hou, Huang et al. 2015), illustrated this by way of growing ≈140 nm length SiO_2 nanorods on Si wafers via a glancing angle deposition technique using an E beam evaporation system. Gold nanoparticles were then sputtered on these rods forming a SERS substrate. The potential to reuse this SERS substrate was shown through multiple detection of monochlorobiphenyl congeners by washing the loaded SERS substrate after each use with acetone. The mechanical strength of a Si wafer and strong mechanical adhesion between silicon based materials and metal nanostructures helped in maintaining the substrate's surface morphology after the repeated washing protocols. Vertically aligned SiO_2 nanowires can also be grown on Si wafers in a patterned manner by chemical etching and the oxide assisted growth method. This is possible by initially using a UV light to selectively expose the surface of a Si wafer covered with a photoresist and a photomask. A metal nanoparticle layer can then be chemically deposited on the exposed layer to act as a catalyst for Si nanowire growth by either chemical etching or oxide assisted growth (Yi, Li et al. 2010). Tao *et al* (Tao, Li et al. 2014) took advantage of the ease of modifying the surface texture of Si wafers and fabricated a SERS substrate by first, texturizing the silicon wafer's surface before hydrothermally growing ZnO nanorods on the texturized surface. The ZnO nanorods were then decorated with Ag nanoparticles by sputtering (Fig. 14). Texturizing the surface triggered the growth of ZnO nanorods at a relatively high density about 1.7 times that grown on a non-

texturized flat surface. This high density is vital for extensive hotspot formation. Furthermore, Si wafers can be designed into a regular network of structured arrays on which a network of periodic spherical nanoparticle arrays can form. According to Zhang's (Zhang, Zhou et al. 2015) research group, this structured arrays with regular network can be formed on a Si wafer by a monolayer colloidal template-induced solution-dipping approach. This can then be followed by the growth of spherical nanoparticle arrays with tuneable gaps between adjacent nanoparticles using a sputtering deposition technique (Fig. 15).

<Insert Fig 14> Fig. 14 Schematic procedure to fabricate the 3D SERS substrate and the related SEM images, **(a)** Top view of texturized Si and side view (the inset) **(b)** ZnO NRs on texturized Si, **(c)** plasmonic structures of ZnO NRs with Ag decoration. From (Tao, Li et al. 2014); Reprinted with permission of Elsevier.

<Insert Fig 15> Fig. 15 Fabrication strategy for periodic spherical nanoparticle arrays. **a)** Monolayer PSs were formed on silicon wafer by self-assembling process. **b)** The monolayer PSs were heated on electric-plate at 120 °C for 25 s. c) 0.5 M Fe $(NO_3)_3$ with addition of 20 $\times 10^{-3}$ M Triton X-100 was dropped onto the surface of monolayer PSs. **d)** After drying at 110 °C for 30 min, the samples were annealing at 400 °C for 2 h to remove the template of PSs, and regular network-structured arrays with prism-like protrusions among three neighbouring holes were formed. **e)** After magnetron sputtering deposition at 50 W for certain time, hexagonal periodic spherical nanoparticle arrays were formed. From (Zhang, Zhou et al. 2015); Reprinted with permission of Wiley online library.

Zhang *et al* used this approach and subsequently coated the spherical nanoparticle arrays with a 30 nm layer of Au to generate a highly sensitive and reproducible SERS substrate (Fig. 16). For R6G, a concentration at 10^{-12} M can be detected on this SERS substrate. This was reported to be due to the hydrophobicity of the fabricated SERS substrate which promoted rapid concentration of analyte solutions onto its surface after surface modification with a perfluorodecanethiol compound. Another property of Si wafers which makes it attractive as a supporting solid platform for SERS substrate fabrication is its ability to generate surface plasmon polaritons. This plasmon (i.e. SPP), when coupled with surface plasmon resonance (SPR), produces a large Raman signal enhancement.

<Insert Fig 16> Fig. 16 FE-SEM images of periodic spherical nanoparticle arrays using regular network-structured arrays as sputtering deposition template. **(b)** is expanded image of **(a).** Scale bars: 500 nm. From (Zhang, Zhou et al. 2015); Reprinted with permission of Wiley online library.

Du *et al* (Du, Zhang et al. 2010) showed this by coating Ag nanoparticles on a Si wafer which was previously patterned with an array of SiO_2 cuboids. A Raman enhancement of $\approx 2 \times 10^9$ was attainable when these two surface plasmons were coupled on the prepared SERS substrate. Some environmental applications of SERS technique involving Si wafer-based SERS substrates are indicated in Table 2.3 below:

<Insert Table 3> Table 3: SERS applications on environmental toxicants using Si wafer-based SERS substrates

3.0 Conclusions

It is apparent from this review that due to their electrical conductivities, electrodes used as solid support platforms on which nanostructures are developed present additional advantages that are usually not found when non-conductive support platforms are used for the fabrication of SERS substrates. For example, these electrodes can support relatively cost-effective, rapid, simple, yet robust electrophoretic and electrochemical nanostructure deposition methods for generating SERS substrates with high densities of uniformly distributed nanostructures as well as nanostructures with different morphologies and substrates possessing numerous hotspots. However, these methods have not been fully explored. In addition, the development of SERS and electrochemical-based dual sensors from conductive nanostructured materials require more investigations. The application of SPR-SPP coupling and semiconductor materials for the improvement of SERS sensitivity also needs to be studied more extensively. Despite their promising properties such as good wettability, numerous hotspot and portability, which make them suitable for in situ detection of environmental toxicants, nanostructured PANI SERS substrates have had limited environmental application in the literature. Advances in this field will therefore be greatly enhanced by exploring the potential advantages of such substrates for environmental applications.

Acknowledgements

We thank Queensland University of Technology (QUT) for the QUT Postgraduate Research Award (QUTPRA) and International HDR Tuition Fee Sponsorship, and the Ghana Atomic Energy Commission (GAEC) for the study leave granted to DKS.

References

Kim, A., Barcelo, S.J., Williams, R.S. and Li, Z. (2012). Melamine sensing in milk products by using surface enhanced Raman scattering. *Analytical chemistry* 84, 9303-9309.

Chan, T.-Y., Liu, T.-Y., Wang, K.-S., Tsai, K.-T., Chen, Z.-X., Chang, Y.-C., Tseng, Y.-Q., Wang, C.-H., Wang, J.-K. and Wang, Y.-L. (2017). SERS Detection of Biomolecules by Highly Sensitive and Reproducible Raman-Enhancing Nanoparticle Array. *Nanoscale research letters* 12, 344.

Bhandari, D., Walworth, M.J. and Sepaniak, M.J. (2009). Dual function surface-enhanced Raman active extractor for the detection of environmental contaminants. *Applied spectroscopy* 63, 571-578.

Tang, X., Dong, R., Yang, L. and Liu, J. (2015). Fabrication of Au nanorod-coated Fe3O4 microspheres as SERS substrate for pesticide analysis by near-infrared excitation. *Journal of Raman Spectroscopy* 46, 470-475.

Li, M., Yang, H., Li, S., Zhao, K., Li, J., Jiang, D., Sun, L. and Deng, A. (2014). Ultrasensitive and quantitative detection of a new β-agonist phenylethanolamine A by a novel immunochromatographic assay based on surface-enhanced Raman scattering (SERS). *Journal of agricultural and food chemistry* 62, 10896-10902.

Pang, S., Yang, T. and He, L. (2016). Review of surface enhanced Raman spectroscopic (SERS) detection of synthetic chemical pesticides. *TrAC Trends in Analytical Chemistry* 85, 73-82.

Izquierdo-Lorenzo, I., Alda, I., Sanchez-Cortes, S. and Garcia-Ramos, J.V. (2012). Adsorption and detection of sport doping drugs on metallic plasmonic nanoparticles of different morphology. *Langmuir* 28, 8891-8901.

Hughes, J., Izake, E.L., Lott, W.B., Ayoko, G.A. and Sillence, M. (2014). Ultra sensitive label free surface enhanced Raman spectroscopy method for the detection of biomolecules. *Talanta* 130, 20-25.

Sivanesan, A., Izake, E.L., Agoston, R., Ayoko, G.A. and Sillence, M. (2015). Reproducible and label-free biosensor for the selective extraction and rapid detection of proteins in biological fluids. *Journal of nanobiotechnology* 13, 43.

Craig, A.P., Franca, A.S. and Irudayaraj, J. (2013). Surface-enhanced Raman spectroscopy applied to food safety. *Annual review of food science and technology* 4, 369-380.

Xie, X., Pu, H. and Sun, D.-W. (2017). Recent advances in nanofabrication techniques for SERS substrates and their applications in food safety analysis. *Critical reviews in food science and nutrition*, 1-14.

Wu, Z., Liu, Y., Zhou, X., Shen, A. and Hu, J. (2013). A "turn-off" SERS-based detection platform for ultrasensitive detection of thrombin based on enzymatic assays. *Biosensors and Bioelectronics* 44, 10-15.

Culha, M. (2013). Surface-enhanced raman scattering: an emerging label-free detection and identification technique for proteins. *Applied spectroscopy* 67, 355-364.

Aroca, R., Alvarez-Puebla, R., Pieczonka, N., Sanchez-Cortez, S. and Garcia-Ramos, J. (2005). Surface-enhanced Raman scattering on colloidal nanostructures. *Advances in colloid and interface science* 116, 45-61.

Kurouski, D. and Van Duyne, R.P. (2015). In situ detection and identification of hair dyes using surface-enhanced Raman spectroscopy (SERS). *Analytical chemistry* 87, 2901-2906.

Schmidt, H., Sowoidnich, K. and Kronfeldt, H.-D. (2010). A prototype hand-held Raman sensor for the in situ characterization of meat quality. *Applied spectroscopy* 64, 888-894.

Xie, W., Qiu, P. and Mao, C. (2011). Bio-imaging, detection and analysis by using nanostructures as SERS substrates. *Journal of Materials Chemistry* 21, 5190-5202.

Ding, S.-Y., Yi, J., Li, J.-F., Ren, B., Wu, D.-Y., Panneerselvam, R. and Tian, Z.-Q. (2016). Nanostructure-based plasmon-enhanced Raman spectroscopy for surface analysis of materials. *Nature Reviews Materials* 1, 16021.

Meyer, S.A., Le Ru, E.C. and Etchegoin, P.G. (2011). Combining surface plasmon resonance (SPR) spectroscopy with surface-enhanced Raman scattering (SERS). *Analytical chemistry* 83, 2337-2344.

Kalachyova, Y., Mares, D., Jerabek, V., Zaruba, K., Ulbrich, P., Lapcak, L., Svorcik, V. and Lyutakov, O. (2016). The effect of silver grating and nanoparticles grafting for LSP–SPP coupling and SERS response intensification. *The Journal of Physical Chemistry C* 120, 10569-10577.

Bernardi, M., Mustafa, J., Neaton, J.B. and Louie, S.G. (2015). Theory and computation of hot carriers generated by surface plasmon polaritons in noble metals. *Nature communications* 6.

Johns, P., Yu, K., Devadas, M.S. and Hartland, G.V. (2016). Role of resonances in the transmission of surface plasmon polaritons between nanostructures. *Acs Nano* 10, 3375-3381.

Willets, K.A. and Van Duyne, R.P. (2007). Localized surface plasmon resonance spectroscopy and sensing. *Annu. Rev. Phys. Chem.* 58, 267-297.

Ren, B., Liu, G.-K., Lian, X.-B., Yang, Z.-L. and Tian, Z.-Q. (2007). Raman spectroscopy on transition metals. *Analytical and bioanalytical chemistry* 388, 29-45.

Kumar, G.P., Shruthi, S., Vibha, B., Reddy, B.A., Kundu, T.K. and Narayana, C. (2007). Hot spots in Ag core-Au shell nanoparticles potent for surface-enhanced Raman scattering studies of biomolecules. *The Journal of Physical Chemistry C* 111, 4388-4392.

Qian, X.-M. and Nie, S. (2008). Single-molecule and single-nanoparticle SERS: from fundamental mechanisms to biomedical applications. *Chemical Society Reviews* 37, 912-920.

Ko, H., Chang, S. and Tsukruk, V.V. (2008). Porous substrates for label-free molecular level detection of nonresonant organic molecules. *Acs Nano* 3, 181-188.

Cardinal, M.F., Vander Ende, E., Hackler, R.A., McAnally, M.O., Stair, P.C., Schatz, G.C. and Van Duyne, R.P. (2017). Expanding applications of SERS through versatile nanomaterials engineering. *Chemical Society Reviews* 46, 3886-3903.

Fateixa, S., Nogueira, H.I. and Trindade, T. (2015). Hybrid nanostructures for SERS: materials development and chemical detection. *Physical Chemistry Chemical Physics* 17, 21046-21071.

Le Ru, E., Blackie, E., Meyer, M. and Etchegoin, P.G. (2007). Surface enhanced Raman scattering enhancement factors: a comprehensive study. *The Journal of Physical Chemistry C* 111, 13794-13803.

Yan, B., Thubagere, A., Premasiri, W.R., Ziegler, L.D., Dal Negro, L. and Reinhard, B.M. (2009). Engineered SERS substrates with multiscale signal enhancement: nanoparticle cluster arrays. *Acs Nano* 3, 1190-1202.

Chen, L., Li, J. and Chen, L. (2014). Colorimetric detection of mercury species based on functionalized gold nanoparticles.

Lin, X.-M., Cui, Y., Xu, Y.-H., Ren, B. and Tian, Z.-Q. (2009). Surface-enhanced Raman spectroscopy: substrate-related issues. *Analytical and bioanalytical chemistry* 394, 1729-1745.

Zou, S. and Schatz, G.C. (2005). Silver nanoparticle array structures that produce giant enhancements in electromagnetic fields. *Chemical Physics Letters* 403, 62-67.

Jiang, J., Bosnick, K., Maillard, M. and Brus, L. (2003). Single molecule Raman spectroscopy at the junctions of large Ag nanocrystals: ACS Publications.

Zhang, J., Zhang, X., Chen, S., Gong, T. and Zhu, Y. (2016). Surface-enhanced Raman scattering properties of multi-walled carbon nanotubes arrays-Ag nanoparticles. *Carbon* 100, 395-407.

Qian, K., Liu, H., Yang, L. and Liu, J. (2012). Designing and fabricating of surface-enhanced Raman scattering substrate with high density hot spots by polyaniline template-assisted self-assembly. *Nanoscale* 4, 6449-6454.

Deng, Y.-L. and Juang, Y.-J. (2014). Black silicon SERS substrate: effect of surface morphology on SERS detection and application of single algal cell analysis. *Biosensors and Bioelectronics* 53, 37-42.

Zhao, W., Xu, Z., Sun, T., Liu, S., Wu, X., Ma, Z., He, J. and Chen, C. (2014). Carbon cloth surface-decorated with silver nanoparticles for surface-enhanced Raman scattering. *Journal of Alloys and Compounds* 584, 635-639.

Bian, J.-C., Chen, Z.-D., Li, Z., Yang, F., He, H.-Y., Wang, J., Tan, J.Z.Y., Zeng, J.-L., Peng, R.-Q. and Zhang, X.-W. (2012). Electrodeposition of hierarchical Ag nanostructures on ITO glass for reproducible and sensitive SERS application. *Applied Surface Science* 258, 6632-6636.

Su, Q., Ma, X., Dong, J., Jiang, C. and Qian, W. (2011). A reproducible SERS substrate based on electrostatically assisted APTES-functionalized surface-assembly of gold nanostars. *ACS applied materials & interfaces* 3, 1873-1879.

Yue, W., Wang, Z., Yang, Y., Chen, L., Syed, A., Wong, K. and Wang, X. (2012). Electron-beam lithography of gold nanostructures for surface-enhanced Raman scattering. *Journal of Micromechanics and Microengineering* 22, 125007.

Coluccio, M.L., Das, G., Mecarini, F., Gentile, F., Pujia, A., Bava, L., Tallerico, R., Candeloro, P., Liberale, C. and De Angelis, F. (2009). Silver-based surface enhanced Raman scattering (SERS) substrate fabrication using nanolithography and site selective electroless deposition. *Microelectronic Engineering* 86, 1085-1088.

Tan, R., Agarwal, A., Balasubramanian, N., Kwong, D., Jiang, Y., Widjaja, E. and Garland, M. (2007). 3D arrays of SERS substrate for ultrasensitive molecular detection. *Sensors and Actuators A: Physical* 139, 36-41.

Whitney, A.V., Myers, B.D. and Van Duyne, R.P. (2004). Sub-100 nm triangular nanopores fabricated with the reactive ion etching variant of nanosphere lithography and angle-resolved nanosphere lithography. *Nano letters* 4, 1507-1511.

Hicks, E.M., Lyandres, O., Hall, W.P., Zou, S., Glucksberg, M.R. and Van Duyne, R.P. (2007). Plasmonic properties of anchored nanoparticles fabricated by reactive ion etching and nanosphere lithography. *The Journal of Physical Chemistry C* 111, 4116-4124.

Liu, M., Sun, L., Cheng, C., Hu, H., Shen, Z. and Fan, H.J. (2011). Highly effective SERS substrates based on an atomic-layer-deposition-tailored nanorod array scaffold. *Nanoscale* 3, 3627-3630.

Zhu, C., Meng, G., Huang, Q., Zhang, Z., Xu, Q., Liu, G., Huang, Z. and Chu, Z. (2011). Ag nanosheet-assembled micro-hemispheres as effective SERS substrates. *Chemical Communications* 47, 2709-2711.

Zhu, S.-Q., Zhang, T., Guo, X.-L., Wang, Q.-L., Liu, X. and Zhang, X.-Y. (2012). Gold nanoparticle thin films fabricated by electrophoretic deposition method for highly sensitive SERS application. *Nanoscale research letters* 7, 613.

Dushaq, G.H., Rasras, M.S. and Nayfeh, A.M. (2017). Distribution and coverage of 40nm gold nano-particles on aluminum and hafnium oxide using electrophoretic method and fabricated MOS structures. *Materials Research Bulletin* 86, 302-307.

Ye, W., Wang, D., Zhang, H., Zhou, F. and Liu, W. (2010). Electrochemical growth of flowerlike gold nanoparticles on polydopamine modified ITO glass for SERS application. *Electrochimica Acta* 55, 2004-2009.

Wang, J., Cao, X., Li, L., Li, T. and Wang, R. (2013). Electrochemical seed-mediated growth of surface-enhanced Raman scattering active Au (111)-like nanoparticles on indium tin oxide electrodes. *The Journal of Physical Chemistry C* 117, 15817-15828.

Jamil, A.K., Izake, E.L., Sivanesan, A., Agoston, R. and Ayoko, G.A. (2015). A homogeneous surface-enhanced Raman scattering platform for ultra-trace detection of trinitrotoluene in the environment. *Analytical Methods* 7, 3863-3868.

Ding, S.-Y., You, E.-M., Tian, Z.-Q. and Moskovits, M. (2017). Electromagnetic theories of surface-enhanced Raman spectroscopy. *Chemical Society Reviews* 46, 4042-4076.

Panneerselvam, R., Liu, G.-K., Wang, Y.-H., Liu, J.-Y., Ding, S.-Y., Li, J.-F., Wu, D.-Y. and Tian, Z.-Q. (2018). Surface-enhanced Raman spectroscopy: bottlenecks and future directions. *Chemical Communications* 54, 10-25.

Nguyen, B.H., Nguyen, V.H. and Tran, H.N. (2016). Rich variety of substrates for surface enhanced Raman spectroscopy. *Advances in Natural Sciences: Nanoscience and Nanotechnology* 7, 033001.

Alvarez-Puebla, R.A. and Liz-Marzan, L.M. (2012). Traps and cages for universal SERS detection. *Chemical Society Reviews* 41, 43-51.

Sun, Z., Du, J. and Jing, C. (2016). Recent progress in detection of mercury using surface enhanced Raman spectroscopy—A review. *Journal of Environmental Sciences* 39, 134-143.

McNay, G., Eustace, D., Smith, W.E., Faulds, K. and Graham, D. (2011). Surface-enhanced Raman scattering (SERS) and surface-enhanced resonance Raman scattering (SERRS): a review of applications. *Applied spectroscopy* 65, 825-837.

Setti, G.O., Mamián-López, M.B., Pessoa, P.R., Poppi, R.J., Joanni, E. and Jesus, D.P. (2015). Sputtered gold-coated ITO nanowires by alternating depositions from Indium and ITO targets for application in surface-enhanced Raman scattering. *Applied Surface Science* 347, 17-22.

Liu, G., Cai, W., Kong, L., Duan, G. and Lü, F. (2010). Vertically cross-linking silver nanoplate arrays with controllable density based on seed-assisted electrochemical growth and their structurally enhanced SERS activity. *Journal of Materials Chemistry* 20, 767-772.

Wang, R., Xu, Y., Wang, C., Zhao, H., Wang, R., Liao, X., Chen, L. and Chen, G. (2015). Fabrication of ITO-rGO/Ag NPs nanocomposite by two-step chronoamperometry electrodeposition and its characterization as SERS substrate. *Applied Surface Science* 349, 805-810.

Zhu, C., Meng, G., Huang, Q., Zhang, Y., Tang, H., Qian, Y., Chen, B. and Wang, X. (2013). Ostwald-Ripening-Induced Growth of Parallel Face-Exposed Ag Nanoplates on Micro-Hemispheres for High SERS Activity. *Chemistry–A European Journal* 19, 9211-9217.

Khlebtsov, B.N., Khanadeev, V.A., Panfilova, E.V., Bratashov, D.N. and Khlebtsov, N.G. (2015). Gold nanoisland films as reproducible SERS substrates for highly sensitive detection of fungicides. *ACS applied materials & interfaces* 7, 6518-6529.

Zhang, H., Wang, J., Wang, H. and Tian, X. (2017). Mace-like gold hollow hierarchical micro/nanostructures fabricated by co-effect of catalytic etching and electrodeposition and their SERS performance. *Materials Research Express* 4, 095009.

Li, Z., Sun, K., Du, Z., Chen, B. and He, X. (2018). Galvanic-Cell-Reaction-Driven Deposition of Large-Area Au Nanourchin Arrays for Surface-Enhanced Raman Scattering. *Nanomaterials* 8, 265.

Sajanlal, P. and Pradeep, T. (2012). Functional hybrid nickel nanostructures as recyclable SERS substrates: detection of explosives and biowarfare agents. *Nanoscale* 4, 3427-3437.

Wang, R., Xu, Y., Wang, R., Wang, C., Zhao, H., Zheng, X., Liao, X. and Cheng, L. (2017). A microfluidic chip based on an ITO support modified with Ag-Au nanocomposites for SERS based determination of melamine. *Microchimica Acta* 184, 279-287.

Zhu, C., Meng, G., Huang, Q. and Huang, Z. (2012). Vertically aligned Ag nanoplate-assembled film as a sensitive and reproducible SERS substrate for the detection of PCB-77. *Journal of hazardous materials* 211, 389-395.

Tran, C.T., Tran, H.T., Bui, H.T., Dang, T.Q. and Nguyen, L.Q. (2017). Determination of low level nitrate/nitrite contamination using SERS-active Ag/ITO substrates coupled to a self-designed Raman spectroscopy system. *Journal of Science: Advanced Materials and Devices*.

Zhang, L. (2013). Self-assembly Ag nanoparticle monolayer film as SERS Substrate for pesticide detection. *Applied Surface Science* 270, 292-294.

Zhang, H., Wang, J., Li, G., Chen, L., Wang, H. and Tian, X. (2019). Fabrication of Ag-nanosheet-assembled hollow tubular array and their SERS effect. *Journal of Alloys and Compounds* 772, 663-668.

Zhang, X., Ji, L., Zhang, S. and Yang, W. (2007). Synthesis of a novel polyaniline-intercalated layered manganese oxide nanocomposite as electrode material for electrochemical capacitor. *Journal of Power Sources* 173, 1017-1023.

Bhadra, S., Khastgir, D., Singha, N.K. and Lee, J.H. (2009). Progress in preparation, processing and applications of polyaniline. *Progress in polymer science* 34, 783-810.

Mostafaei, A. and Zolriasatein, A. (2012). Synthesis and characterization of conducting polyaniline nanocomposites containing ZnO nanorods. *Progress in Natural Science: Materials International* 22, 273-280.

Xu, P., Mack, N.H., Jeon, S.-H., Doorn, S.K., Han, X. and Wang, H.-L. (2010). Facile fabrication of homogeneous 3D silver nanostructures on gold-supported polyaniline membranes as promising SERS substrates. *Langmuir* 26, 8882-8886.

Li, S., Xiong, L., Liu, S. and Xu, P. (2014). Fast fabrication of homogeneous Ag nanostructures on dual-acid doped polyaniline for SERS applications. *RSC Advances* 4, 16121-16126.

He, J., Han, X., Yan, J., Kang, L., Zhang, B., Du, Y., Dong, C., Wang, H.-L. and Xu, P. (2012). Fast fabrication of homogeneous silver nanostructures on hydrazine treated polyaniline films for SERS applications. *CrystEngComm* 14, 4952-4954.

Yan, J., Han, X., He, J., Kang, L., Zhang, B., Du, Y., Zhao, H., Dong, C., Wang, H.-L. and Xu, P. (2012). Highly sensitive surface-enhanced Raman spectroscopy (SERS) platforms based on silver nanostructures fabricated on polyaniline membrane surfaces. *ACS applied materials & interfaces* 4, 2752-2756.

Mondal, S., Rana, U. and Malik, S. (2015). Facile decoration of polyaniline fiber with Ag nanoparticles for recyclable SERS substrate. *ACS applied materials & interfaces* 7, 10457-10465.

Wang, X., Shen, Y., Xie, A. and Chen, S. (2013). One-step synthesis of Ag@ PANI nanocomposites and their application to detection of mercury. *Materials Chemistry and Physics* 140, 487-492.

Wang, X., Shen, Y., Xie, A., Li, S., Cai, Y., Wang, Y. and Shu, H. (2011). Assembly of dandelion-like Au/PANI nanocomposites and their application as SERS nanosensors. *Biosensors and Bioelectronics* 26, 3063-3067.

Sun, Y., Liu, K., Miao, J., Wang, Z., Tian, B., Zhang, L., Li, Q., Fan, S. and Jiang, K. (2010). Highly sensitive surface-enhanced Raman scattering substrate made from superaligned carbon nanotubes. *Nano letters* 10, 1747-1753.

Dresselhaus, M.S. and Terrones, M. (2013). Carbon-based nanomaterials from a historical perspective. *Proceedings of the IEEE* 101, 1522-1535.

Chen, Y.-C., Young, R.J., Macpherson, J.V. and Wilson, N.R. (2007). Single-walled carbon nanotube networks decorated with silver nanoparticles: a novel graded SERS substrate. *The Journal of Physical Chemistry C* 111, 16167-16173.

Halvorson, R.A. and Vikesland, P.J. (2010). Surface-enhanced Raman spectroscopy (SERS) for environmental analyses. *Environmental science & technology* 44, 7749-7755.

Beqa, L., Singh, A.K., Fan, Z., Senapati, D. and Ray, P.C. (2011). Chemically attached gold nanoparticle–carbon nanotube hybrids for highly sensitive SERS substrate. *Chemical Physics Letters* 512, 237-242.

Jiang, W.F., Zhang, Y.F., Wang, Y.S., Xu, L. and Li, X.J. (2011). SERS activity of Au nanoparticles coated on an array of carbon nanotube nested into silicon nanoporous pillar. *Applied Surface Science* 258, 1662-1665.

Bui, M.-P.N., Lee, S., Han, K.N., Pham, X.-H., Li, C.A., Choo, J. and Seong, G.H. (2009). Electrochemical patterning of gold nanoparticles on transparent single-walled carbon nanotube films. *Chemical Communications*, 5549-5551.

Duy, P.K., Yen, P.T.H., Chun, S., Ha, V.T.T. and Chung, H. (2016). Carbon fiber cloth-supported Au nanodendrites as a rugged surface-enhanced Raman scattering substrate and electrochemical sensing platform. *Sensors and Actuators B: Chemical* 225, 377-383.

Wang, X., Zhou, L., Wei, G., Jiang, T. and Zhou, J. (2016). SERS-based immunoassay using a core–shell SiO 2@ Ag immune probe and Ag-decorated NiCo 2 O 4 nanorods immune substrate. *RSC Advances* 6, 708-715.

Xie, Y., Jin, Y., Zhou, Y. and Wang, Y. (2014). SERS activity of self-cleaning silver/titania nanoarray. *Applied Surface Science* 313, 549-557.

Li, X., Hu, H., Li, D., Shen, Z., Xiong, Q., Li, S. and Fan, H.J. (2012). Ordered array of gold semishells on TiO2 spheres: an ultrasensitive and recyclable SERS substrate. *ACS applied materials & interfaces* 4, 2180-2185.

Deng, S., Fan, H., Zhang, X., Loh, K.P., Cheng, C., Sow, C. and Foo, Y. (2009). An effective surface-enhanced Raman scattering template based on a Ag nanocluster–ZnO nanowire array. *Nanotechnology* 20, 175705.

Rodriguez-Fernandez, D., Langer, J., Henriksen-Lacey, M. and Liz-Marzán, L.M. (2015). Hybrid Au–SiO2 Core–Satellite Colloids as Switchable SERS Tags. *Chemistry of Materials* 27, 2540-2545.

Yang, L., Ruan, W., Jiang, X., Zhao, B., Xu, W. and Lombardi, J.R. (2008). Contribution of ZnO to charge-transfer induced surface-enhanced Raman scattering in Au/ZnO/PATP assembly. *The Journal of Physical Chemistry C* 113, 117-120.

Wang, Z., Meng, G., Huang, Z., Li, Z. and Zhou, Q. (2014). Ag-nanoparticle-decorated porous ZnO-nanosheets grafted on a carbon fiber cloth as effective SERS substrates. *Nanoscale* 6, 15280-15285.

Huang, J., Chen, F., Zhang, Q., Zhan, Y., Ma, D., Xu, K. and Zhao, Y. (2015). 3D silver nanoparticles decorated zinc oxide/silicon heterostructured nanomace arrays as high-

performance surface-enhanced Raman scattering substrates. *ACS applied materials & interfaces* 7, 5725-5735.

Halouzka, V., Halouzkova, B., Jirovsky, D., Hemzal, D., Ondra, P., Siranidi, E., Kontos, A.G., Falaras, P. and Hrbac, J. (2017). Copper nanowire coated carbon fibers as efficient substrates for detecting designer drugs using SERS. *Talanta* 165, 384-390.

Tran, M., Fallatah, A., Whale, A. and Padalkar, S. (2018). Utilization of Inexpensive Carbon-Based Substrates as Platforms for Sensing. *Sensors* 18, 2444.

Huang, C., Xu, C., Lu, J., Li, Z. and Tian, Z. (2016). 3D Ag/ZnO hybrids for sensitive surface-enhanced Raman scattering detection. *Applied Surface Science* 365, 291-295.

Zhang, K., Ji, J., Fang, X., Yan, L. and Liu, B. (2015). Carbon nanotube/gold nanoparticle composite-coated membrane as a facile plasmon-enhanced interface for sensitive SERS sensing. *Analyst* 140, 134-139.

Mbah, J., Moorer, K., Pacheco-Londoño, L., Hernandez-Rivera, S. and Cruz, G. (2013). A rapid technique for synthesis of metallic nanoparticles for surface enhanced Raman spectroscopy. *Journal of Raman Spectroscopy* 44, 723-726.

Kang, Y., Wu, T., Han, X., Gu, H. and Zhang, X. (2018). A needle-like reusable surface-enhanced Raman scattering substrate, and its application to the determination of acetamiprid by combining SERS and thin-layer chromatography. *Microchimica Acta* 185, 504.

Dinh, N.X., Huy, T.Q. and Le, A.-T. (2016). Multiwalled carbon nanotubes/silver nanocomposite as effective SERS platform for detection of methylene blue dye in water. *Journal of Science: Advanced Materials and Devices* 1, 84-89.

Jiang, Z., Jiang, X., Su, S., Wei, X., Lee, S. and He, Y. (2012). Silicon-based reproducible and active surface-enhanced Raman scattering substrates for sensitive, specific, and multiplex DNA detection. *Applied Physics Letters* 100, 203104.

Chursanova, M., Germash, L., Yukhymchuk, V., Dzhagan, V., Khodasevich, I. and Cojoc, D. (2010). Optimization of porous silicon preparation technology for SERS applications. *Applied Surface Science* 256, 3369-3373.

Peng, F., Su, Y., Zhong, Y., Fan, C., Lee, S.-T. and He, Y. (2014). Silicon nanomaterials platform for bioimaging, biosensing, and cancer therapy. *Accounts of Chemical Research* 47, 612-623.

He, Y., Fan, C. and Lee, S.-T. (2010). Silicon nanostructures for bioapplications. *Nano Today* 5, 282-295.

Shao, Q., Que, R., Shao, M., Cheng, L. and Lee, S.T. (2012). Copper Nanoparticles Grafted on a Silicon Wafer and Their Excellent Surface-Enhanced Raman Scattering. *Advanced Functional Materials* 22, 2067-2070.

Giorgis, F., Descrovi, E., Chiodoni, A., Froner, E., Scarpa, M., Venturello, A. and Geobaldo, F. (2008). Porous silicon as efficient surface enhanced Raman scattering (SERS) substrate. *Applied Surface Science* 254, 7494-7497.

Panarin, A.Y., Terekhov, S., Kholostov, K. and Bondarenko, V. (2010). SERS-active substrates based on n-type porous silicon. *Applied Surface Science* 256, 6969-6976.

Rajkumar, K., Jayram, N.D., Mangalaraj, D. and Kumar, R.T.R. (2016). One step 'dip'and 'use'Ag nanostructured thin films for ultrahigh sensitive SERS Detection. *Materials Science and Engineering: C* 68, 831-836.

Alexander, K.D., Hampton, M.J., Zhang, S., Dhawan, A., Xu, H. and Lopez, R. (2009). A high-throughput method for controlled hot-spot fabrication in SERS-active gold nanoparticle dimer arrays. *Journal of Raman Spectroscopy* 40, 2171-2175.

Fang, C., Agarwal, A., Buddharaju, K.D., Khalid, N.M., Salim, S.M., Widjaja, E., Garland, M.V., Balasubramanian, N. and Kwong, D.-L. (2008). DNA detection using nanostructured SERS substrates with Rhodamine B as Raman label. *Biosensors and Bioelectronics* 24, 216-221.

Atay, T., Song, J.-H. and Nurmikko, A.V. (2004). Strongly interacting plasmon nanoparticle pairs: from dipole− dipole interaction to conductively coupled regime. *Nano letters* 4, 1627-1631.

Su, K.-H., Wei, Q.-H., Zhang, X., Mock, J., Smith, D.R. and Schultz, S. (2003). Interparticle coupling effects on plasmon resonances of nanogold particles. *Nano letters* 3, 1087-1090.

Hou, M., Huang, Y., Ma, L. and Zhang, Z. (2015). Sensitivity and Reusability of SiO2 NRs@ Au NPs SERS Substrate in Trace Monochlorobiphenyl Detection. *Nanoscale research letters* 10, 444.

Yi, C., Li, C.-W., Fu, H., Zhang, M., Qi, S., Wong, N.-B., Lee, S.-T. and Yang, M. (2010). Patterned growth of vertically aligned silicon nanowire arrays for label-free DNA detection using surface-enhanced Raman spectroscopy. *Analytical and bioanalytical chemistry* 397, 3143-3150.

Tao, Q., Li, S., Zhang, Q., Kang, D., Yang, J., Qiu, W. and Liu, K. (2014). Controlled growth of ZnO nanorods on textured silicon wafer and the application for highly effective and recyclable SERS substrate by decorating Ag nanoparticles. *Materials Research Bulletin* 54, 6-12.

Zhang, H., Zhou, F., Liu, M., Liu, D., Men, D., Cai, W., Duan, G. and Li, Y. (2015). Spherical nanoparticle arrays with tunable nanogaps and their hydrophobicity enhanced rapid SERS detection by localized concentration of droplet evaporation. *Advanced Materials Interfaces* 2.

Du, L., Zhang, X., Mei, T. and Yuan, X. (2010). Localized surface plasmons, surface plasmon polaritons, and their coupling in 2D metallic array for SERS. *Optics express* 18, 1959-1965.

Yang, Y. and Meng, G. (2010). Ag dendritic nanostructures for rapid detection of polychlorinated biphenyls based on surface-enhanced Raman scattering effect. *Journal of Applied Physics* 107, 044315.

Zuo, Z., Zhu, K., Ning, L., Cui, G., Qu, J., Cheng, Y., Wang, J., Shi, Y., Xu, D. and Xin, Y. (2015). Highly sensitive surface enhanced Raman scattering substrates based on Ag decorated Si nanocone arrays and their application in trace dimethyl phthalate detection. *Applied Surface Science* 325, 45-51.

Liu, L., Wu, F., Xu, D., Li, N. and Lu, N. (2018). Space confined electroless deposition of silver nanoparticles for highly-uniform SERS detection. *Sensors and Actuators B: Chemical* 255, 1401-1406.

Akin, M.S., Yilmaz, M., Babur, E., Ozdemir, B., Erdogan, H., Tamer, U. and Demirel, G. (2014). Large area uniform deposition of silver nanoparticles through bio-inspired polydopamine coating on silicon nanowire arrays for practical SERS applications. *Journal of Materials Chemistry B* 2, 4894-4900.

Tang, J.-j., Sun, J.-f., Lui, R., Zhang, Z.-m., Liu, J.-f. and Xie, J.-w. (2016). New surface-enhanced raman sensing chip designed for on-site detection of active ricin in complex matrices based on specific depurination. *ACS applied materials & interfaces* 8, 2449-2455.

Zhang, Z., Yu, Q., Li, H., Mustapha, A. and Lin, M. (2015). Standing gold nanorod arrays as reproducible SERS substrates for measurement of pesticides in apple juice and vegetables. *Journal of food science* 80, N450-N458.

Han, X., Wang, H., Ou, X. and Zhang, X. (2012). Highly sensitive, reproducible, and stable SERS sensors based on well-controlled silver nanoparticle-decorated silicon nanowire building blocks. *Journal of Materials Chemistry* 22, 14127-14132.

Sinha, G., Depero, L.E. and Alessandri, I. (2011). Recyclable SERS substrates based on Au-coated ZnO nanorods. *ACS applied materials & interfaces* 3, 2557-2563.

Liu, B., Zhou, P., Liu, X., Sun, X., Li, H. and Lin, M. (2013). Detection of pesticides in fruits by surface-enhanced Raman spectroscopy coupled with gold nanostructures. *Food and Bioprocess Technology* 6, 710-718.

Guo, K., Xiao, R., Zhang, X., Wang, C., Liu, Q., Rong, Z., Ye, L. and Chen, S. (2015). Silver nanopartical over AuFON substrate for enhanced raman readout and their application in pesticide monitoring. *Molecules* 20, 6299-6309.

Tang, H., Meng, G., Huang, Q., Zhang, Z., Huang, Z. and Zhu, C. (2012). Arrays of cone-shaped ZnO nanorods decorated with Ag nanoparticles as 3D surface-enhanced Raman scattering substrates for rapid detection of trace polychlorinated biphenyls. *Advanced Functional Materials* 22, 218-224.

Kwon, Y.H., Sowoidnich, K., Schmidt, H. and Kronfeldt, H.D. (2012). Application of calixarene to high active surface-enhanced Raman scattering (SERS) substrates suitable for in situ detection of polycyclic aromatic hydrocarbons (PAHs) in seawater. *Journal of Raman Spectroscopy* 43, 1003-1009.

Tu, X., Li, Z., Lu, J., Zhang, Y., Yin, G., Wang, W. and He, D. (2018). In situ preparation of Ag nanoparticles on silicon wafer as highly sensitive SERS substrate. *RSC Advances* 8, 2887-2891.

Zhang, X., Xiao, X., Dai, Z., Wu, W., Zhang, X., Fu, L. and Jiang, C. (2017). Ultrasensitive SERS performance in 3D “sunflower-like” nanoarrays decorated with Ag nanoparticles. *Nanoscale* 9, 3114-3120.

Kumar, S., Goel, P. and Singh, J.P. (2017). Flexible and robust SERS active substrates for conformal rapid detection of pesticide residues from fruits. *Sensors and Actuators B: Chemical* 241, 577-583.

Shi, Y., Chen, N., Su, Y., Wang, H. and He, Y. (2018). Silicon nanohybrid-based SERS chips armed with an internal standard for broad-range, sensitive and reproducible simultaneous quantification of lead (ii) and mercury (ii) in real systems. *Nanoscale* 10, 4010-4018.

Fabrication of nanostructured SERS substrates on conductive solid platforms for environmental application

Legend to Figures

Fig. 1 Schematic illustration of (A) surface plasmon polariton and (B) localised surface plasmon

Fig. 2 Schematic representation of SERS phenomenon for an analyte on Au nanoparticles.

Fig. 3 Number of publications per year from 2009 – 2018 period searched through Web of Science using the keywords "SERS Substrate and fabrication" and "SERS and nanostructures"

Fig. 4 FSEM images of GNPs immobilised on ITO by electrophoresis at ≤ 2mins **(a and b),** 8 mins **(c)** and **(d)** High resolution image at 8 mins. Red circles indicate sub-10-nm gaps between neighbouring nanoparticles. From Reference(Zhu, Zhang et al. 2012); Reprinted with permission of Springer.

Fig. 5 A schematic illustration of the preferential nucleation and oriented growth for cross-linking Ag nanoplate arrays: (a) random-oriented Ag seeds laying on the ITO substrate, and Ag nuclei are preferentially formed on some <110>-oriented seeds (see arrow's marks); (b) oriented growth of the nuclei along the fastest <110> within (111) plane under a low deposition current density; (c) cross-linking Ag nanoplate array structure is formed and standing on the substrate vertically. From (Liu, Cai et al. 2010); Reprinted with permission of The Royal Society of Chemistry.

Fig. 6 (a–c) SEM images of Ag microhemispheres at different magnification. The inset in (a) is the SEM side view of the microhemispheres. (d and e) Cross-sectional SEM views of a microhemisphere. (f) The size distribution of the Ag micro-hemispheres in (a). (g and h) Differently magnified SEM images of an imperfect Ag microhemisphere. (i) TEM image of

fan-shaped pieces broken off from an imperfect Ag micro-hemisphere as shown in (g). The inset in (i) is the SAED pattern from the black circle. (j) SERS spectra of 10−11 M R6G from five randomly chosen individual micro-hemispheres. From (Zhu, Meng et al. 2011); Reprinted with permission of The Royal Society of Chemistry.

Fig. 7 A schematic illustration of the seed mediated two step electrochemical approach for deposition of AuNPs on ITO and its utilization for the detection of 4-Mercaptobenzoic acid (p-MBA). From (Wang, Cao et al. 2013); Reprinted with permission of The American Chemical Society.

Fig.8 SEM images of **(a)** Au nanoparticles grown on a PANI membrane (doped by citric acid) by immersing the PANI membrane in 10 mM $AuCl_3$ aqueous solution for 10 s, and the Ag nanostructures produced by immersing the Au nanolayer-supported PANI membrane in 50 mM $AgNO_3$ aqueous solution for **(b)** 10 s**, (c)** 30 s, **(d)** 1 min, **(e)** 10 min, and **(f)** 60 min. The scale bar is 500 nm. From (Xu, Mack et al. 2010); Reprinted with permission of The American Chemical Society.

Fig. 9 SEM images of Ag nanostructures produced on hydrazine treated PANI films at a reaction time of 30 s **(a)**, 1 min **(b)**, 2 min **(c)** and 5 min **(d)**, with lactic acid present and 30 s **(e)**, 1 min **(f)**, 2 min **(g)** and 5 min **(h),** with succinic acid present in the $AgNO_3$ solution. Scale bar: 3 mm. From (He, Han et al. 2012); Reprinted with permission of The Royal Society of Chemistry

Fig. 10 SEM images of Ag nanostructures produced on the camphorsulfonic-acid-doped PANI membranes, with **(a, b)** succinic acid, **(c, d)** lactic acid, and **(e, f)** camphorsulfonic acid present in the AgNO3 solution. From (Yan, Han et al. 2012); Reprinted with permission of The American Chemical Society

Fig. 11 FE-SEM images of gold nanoparticles patterned onto SWCNT films by electrochemical deposition. The deposited charges for **(A), (B),** and **(C)** were 1 mC, 10 mC, and 30 mC, respectively. The scale bars in the left, middle and right columns are 100 mm, 10 mm and 1 mm, respectively. From (Bui, Lee et al. 2009); Reprinted with permission of The Royal Society of Chemistry.

Fig. 12 (A) ZnO-mesoporous-NSs grafted on CFs **(a)** Top-view SEM image. The lower-left inset is an optical photo of a piece of ZnO-mesoporous-NSs@CFC. **(b)** Magnified SEM observation on two adjacent CFs grafted with ZnO-mesoporous-NSs. **(c)** Close-up SEM view of a few ZnO-mesoporous-NSs. **(d)** TEM image of a single ZnO-mesoporous-NS and its corresponding selected area electron diffraction pattern; (B) SEM images of Ag-NP decorated on ZnO-mesoporous-NSs with (a) 20 s, (b) 60 s, (c) 120 s and (d) 180 s Ag sputtering time. From (Wang, Meng et al. 2014); Reprinted with permission of The Royal Society of Chemistry.

Fig. 13 (a) Scanning electron micrograph of an array of nanoholes patterned into a Si wafer after Cr deposition, removal of PLGA posts, and reactive ion etching. **(b)** Aspect of whole wafer patterned with nanoholes. From (Alexander, Hampton et al. 2009); Reprinted with permission of Wiley online library.

Fig. 14 Schematic procedure to fabricate the 3D SERS substrate and the related SEM images, **(a)** Top view of texturized Si and side view (the inset) **(b)** ZnO NRs on texturized Si, **(c)** plasmonic structures of ZnO NRs with Ag decoration. From (Tao, Li et al. 2014); Reprinted with permission of Elsevier.

Fig. 15 Fabrication strategy for periodic spherical nanoparticle arrays. **a)** Monolayer PSs were formed on silicon wafer by self-assembling process. **b)** The monolayer PSs were heated on electric-plate at 120 °C for 25 s. c) 0.5 M Fe $(NO_3)_3$ with addition of 20×10^{-3} M Triton X-100 was dropped onto the surface of monolayer PSs. **d)** After drying at 110 °C for 30 min, the

samples were annealing at 400 °C for 2 h to remove the template of PSs, and regular network-structured arrays with prism-like protrusions among three neighbouring holes were formed. **e)** After magnetron sputtering deposition at 50 W for certain time, hexagonal periodic spherical nanoparticle arrays were formed. From (Zhang, Zhou et al. 2015); Reprinted with permission of Wiley online library.

Fig. 16 FE-SEM images of periodic spherical nanoparticle arrays using regular network-structured arrays as sputtering deposition template **(b)** is expanded image of **(a)** Scale bars: 500 nm. From (Zhang, Zhou et al. 2015); Reprinted with permission of Wiley online library.

Figures 1-16

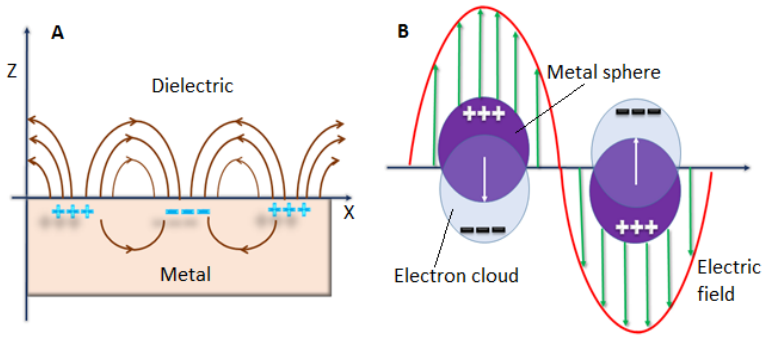

Fig 1

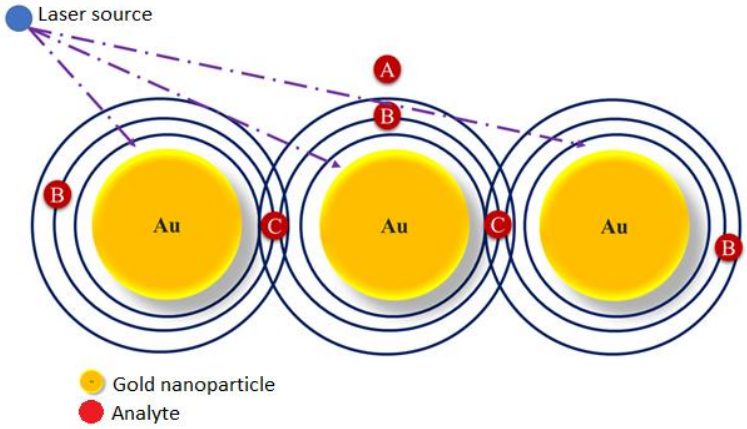

Fig. 2.

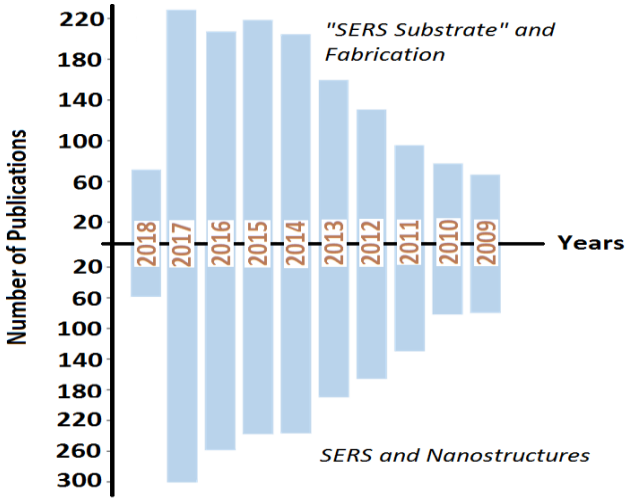
"SERS Substrate" and Fabrication
SERS and Nanostructures
Number of Publications
Years
220
180
140
100
60
20
20
60
100
140
180
220
260
300
2018
2017
2016
2015
2014
2013
2012
2011
2010
2009

Fig. 3

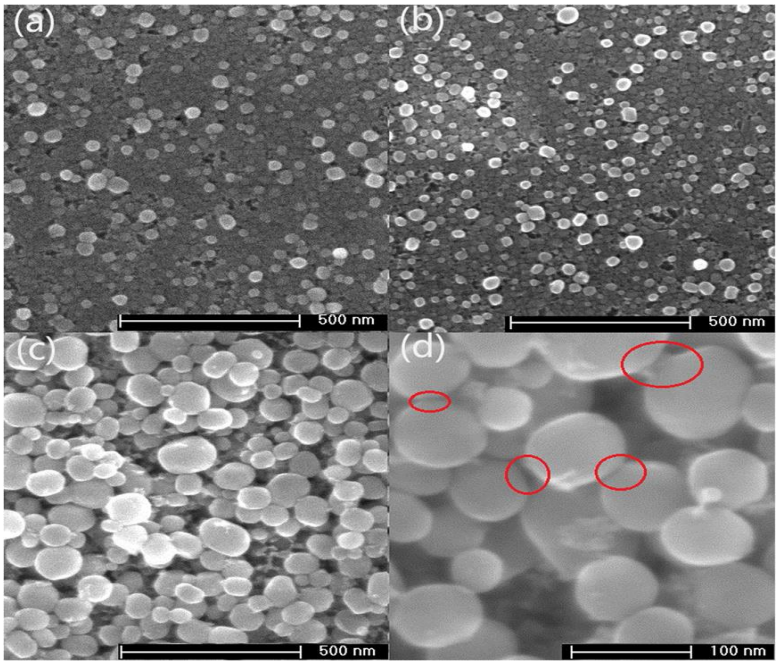
(a)
(b)
(c)
(d)
500 nm
500 nm
500 nm
100 nm

Fig. 4

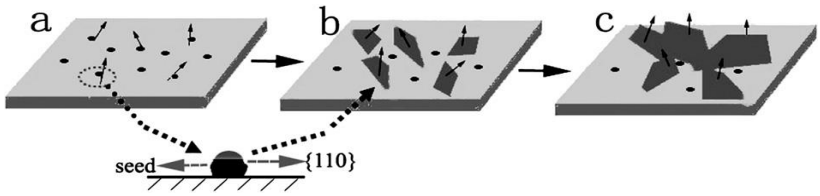

Fig. 5

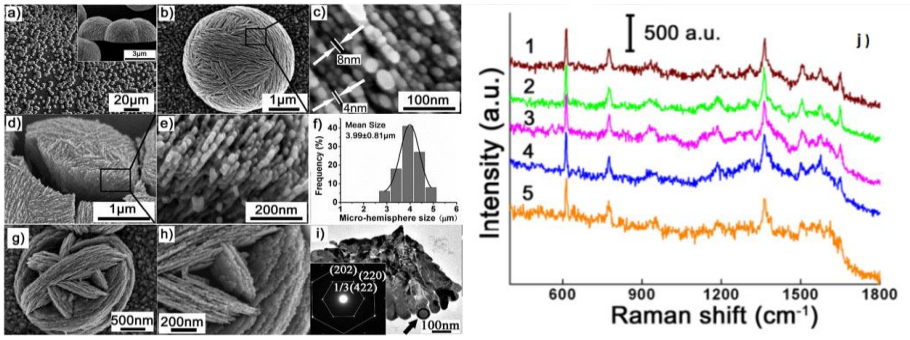

Fig. 6

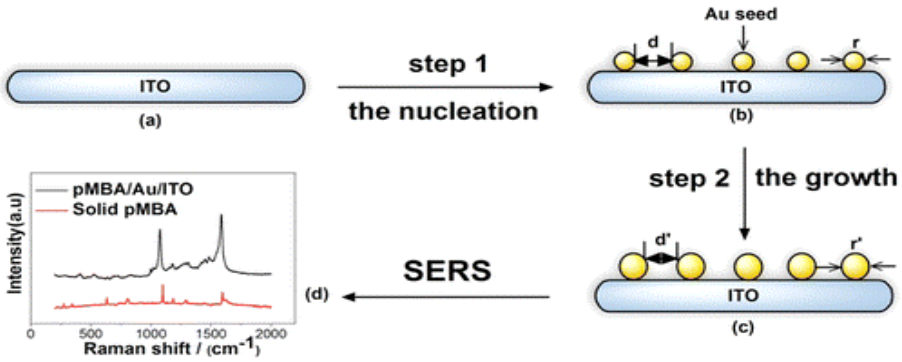

Fig. 7

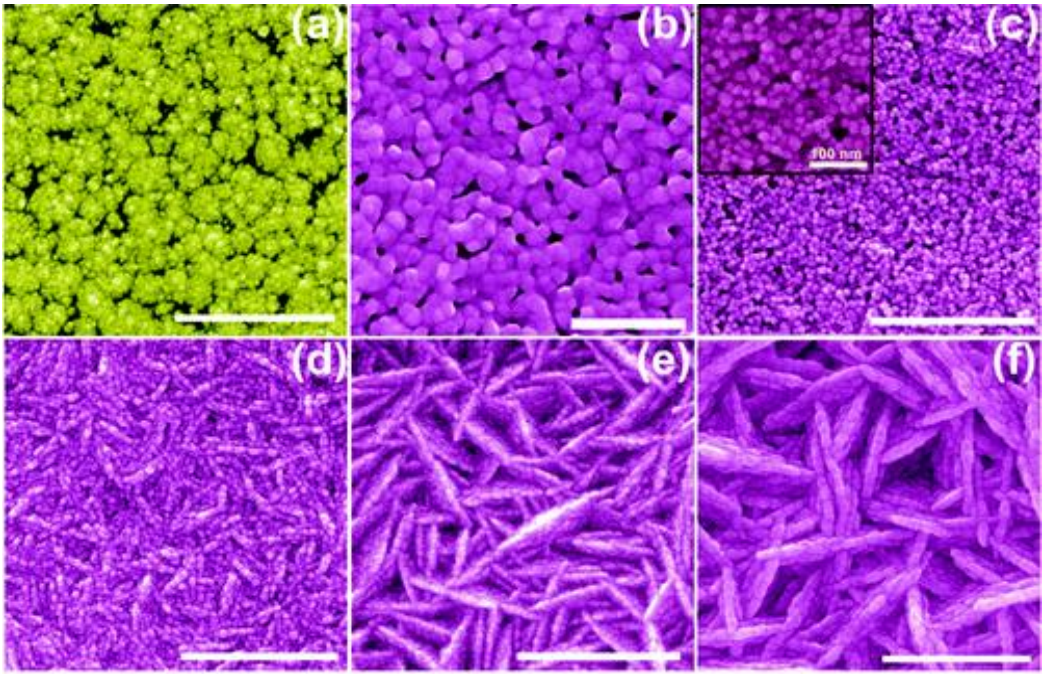

Fig.8

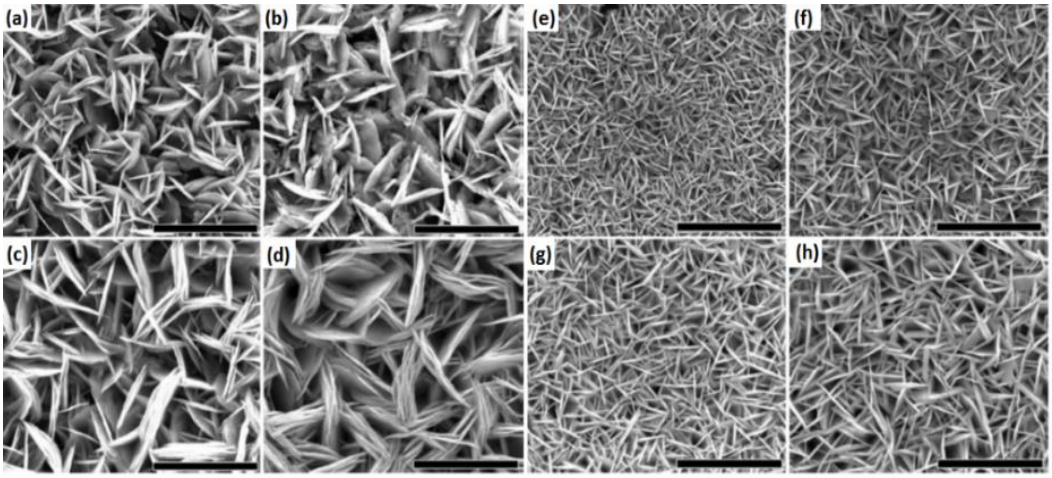

Fig. 9

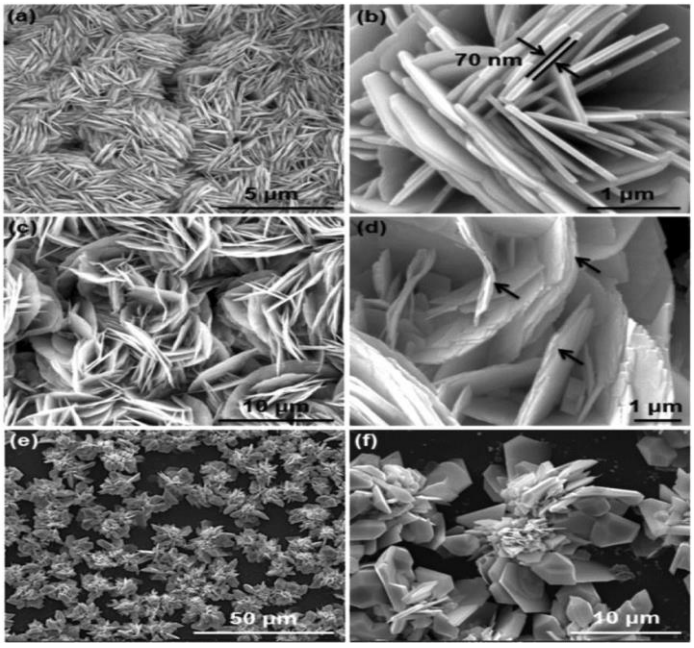

Fig. 10

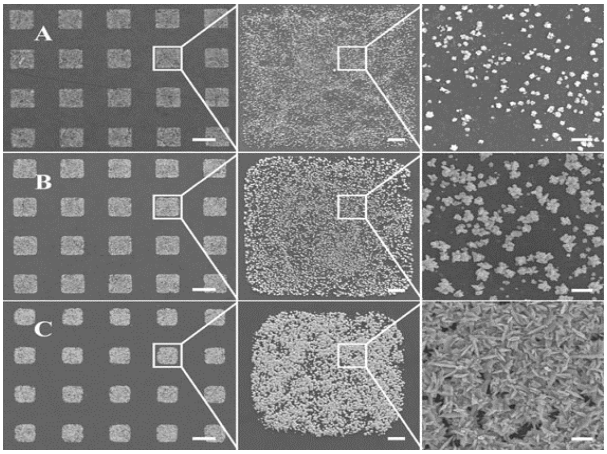

Fig. 11

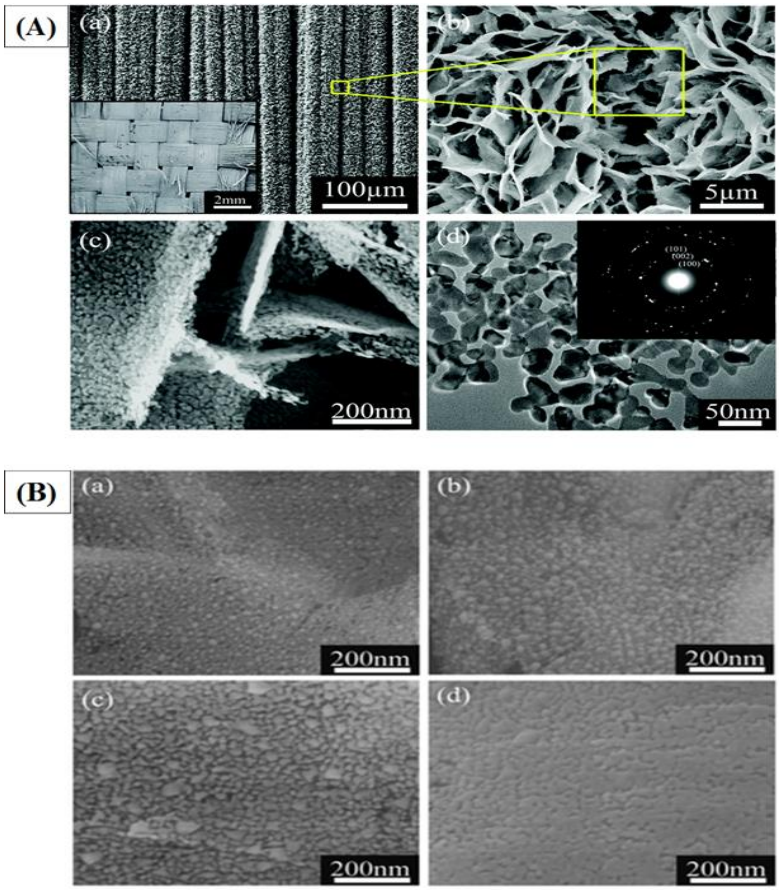
(A)
(a)
2mm
100μm
(b)
5μm
(c)
200nm
(d)
50nm
(B)
(a)
200nm
(b)
200nm
(c)
200nm
(d)
200nm

Fig. 12

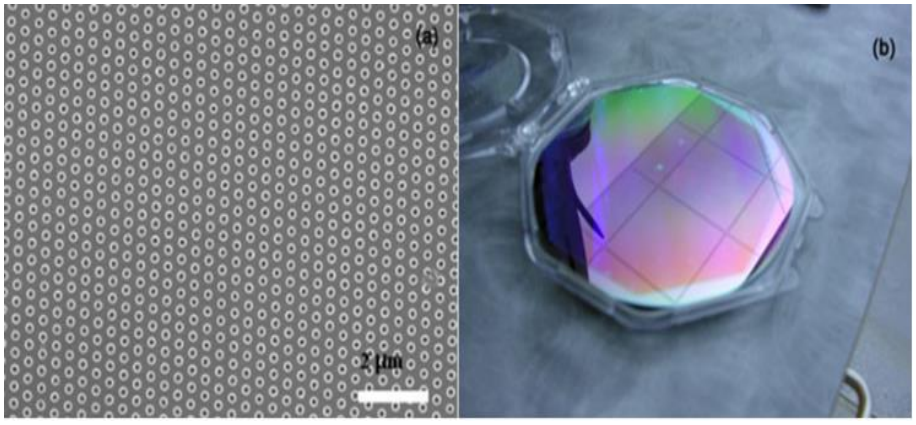
(a)
(b)

Fig. 13

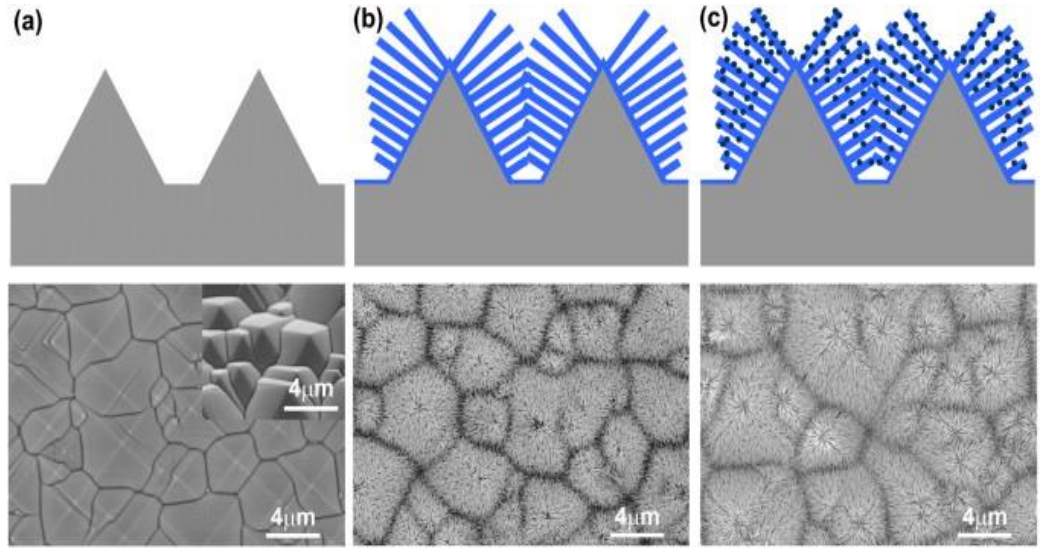
(a)
(b)
(c)
4μm
4μm
4μm
4μm

Fig. 14

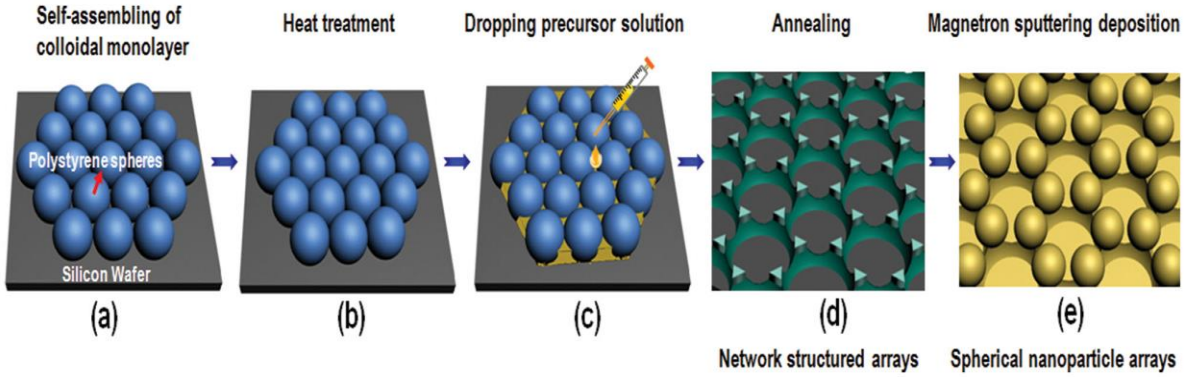
Self-assembling of colloidal monolayer
Heat treatment
Dropping precursor solution
Annealing
Magnetron sputtering deposition
Polystyrene spheres
Silicon Wafer
(a)
(b)
(c)
(d)
(e)
Network structured arrays
Spherical nanoparticle arrays

Fig. 15

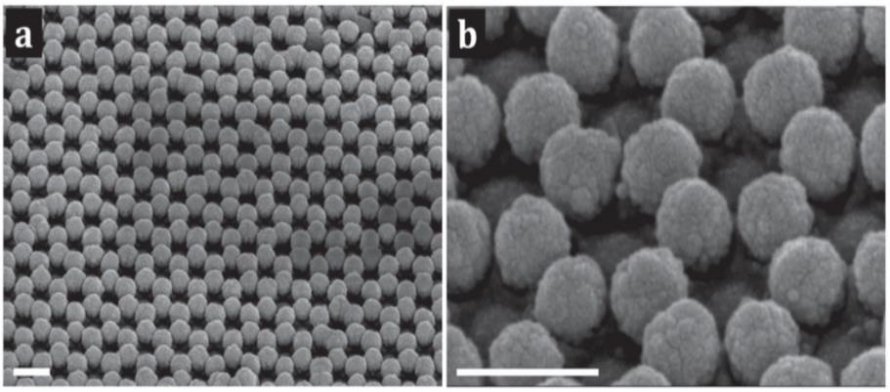

Fig. 16

Fabrication of nanostructured SERS substrates on conductive solid platforms for environmental application

Daniel K. Sarfo, Emad L. Izake, Anthony P. O'Mullane, and Godwin A. Ayoko*

Queensland University of Technology(QUT), School of Chemistry, Physics and Mechanical Engineering, 2 George street, QLD 4001, Australia.

*Corresponding Author

E-mail: g.ayoko@qut.edu.au

Legend to Tables

Table 1: SERS applications on environmental toxicants using ITO-based substrates

Table 2: SERS applications on environmental toxicants using carbon-based substrates

Table 3: SERS applications on environmental toxicants using Si wafer-based substrates

Table 1:

Material	Fabrication method	Application	LOD	References
Au nanosheets on ITO glass	Electrodeposition followed by Ostwald-ripening-induced growth	2-chlorobiphenyl (PCB-1) and 3,3',4,4'-tetrachlorobiphenyl (PCB-77)	10 nM (PCB-1) and 10 nM (PCB-77)	(Zhu, Meng et al. 2013)
Au nano islands on ITO glass	Wet chemistry using 3-mercaptopropyl) trimethoxysilane and ascorbic acid	Thiram	5 ng/cm^2	(Khlebtsov, Khanadeev et al. 2015)
Ag nanosheet-assembled micro-hemispheres on ITO-glass	Electrodeposition	Polychlorinated biphenyls (PCB-1 and PCB-77) detection	0.3 µM (PCB-77) and 30 µM (PCB-1)	(Zhu, Meng et al. 2011)
ITO-glass modified with hybrid nickel nanostructures	Reduction of Ni to Ni nanowires (Ni NW) and Ni nanocarpets (Ni NC) in hydrazine hydrate followed by immersion of Ni NW and Ni NC in $HAuCl_4$, H_2PdCl_4 and H_2PtCl_6 to form hybrid nickel nanostructures	2,4-dinitrotoluene (DNT), Trinitrotoluene (TNT) and Hexahydro-1,3,5-triazine (RDX)	0.1µM (DNT), 0.1µM (TNT) and 1µM (RDX)	(Sajanlal and Pradeep 2012)
Mace-like gold hollow hierarchical micro/nanostructures on ZnO bearing ITO	Coating of ITO with ZnO film via atomic layer deposition followed by electrochemical growth of ZnO NRs. Au layer of 15 nm thickness was sputtered on the ZnO NRs	Rhodamine 6G	0.1 nM	(Zhang, Wang et al. 2017)
Au nanourchin Arrays on ITO	Spin coating of ITO with Ag seed followed by deposition of Au nanourchins via a galvanic-Cell-reaction technique	PCB-77	5 µM	(Li, Sun et al. 2018)
Mace-like gold hollow hierarchical micro/nanostructures on ZnO bearing ITO	Coating of ITO with ZnO film via atomic layer deposition followed by electrochemical growth of ZnO NRs. Au layer of 15 nm	Rhodamine 6G	0.1 nM	(Zhang, Wang, Wang and Tian 2017)

	thickness was sputtered on the ZnO NRs			
Au nanourchin Arrays on ITO	Spin coating of ITO with Ag seed followed by deposition of Au nanourchins via a galvanic-Cell-reaction technique	PCB-77	5 µM	(Li, Sun, Du, Chen and He 2018)
Microfluidic chip with an Ag-Au nanocomposites modified ITO	Electrodeposition and galvanic displacement reaction	Melamine detection	0.1 nM	(Wang, Xu et al. 2017)
Vertically aligned Ag nanoplate on ITO	Spin-coating of Ag seeds followed by electrodeposition	PCB-77	1 µM	(Zhu, Meng et al. 2012)
ITO modified with Ag NP	Electrodeposition	Nitrate and Nitrite detection	1 ppm (nitrate) and 0.1 ppm (nitrite)	(Tran, Tran et al. 2017)
Monolayer film of AgNP on ITO	Functionalisation of ITO with 3-aminopropyltrimethoxysilane followed by Self-assembly of AgNP	Methyl-parathion	0.1 µM	(Zhang 2013)
ITO with Ag-nanosheet-assembled hollow tubular array	Electrodeposition of ZnO NRs on ITO covered with ZnO seed layer followed by Au sputtering on ZnO NRs. Ag-nanosheet hollow tubular array were then electrodeposited.	Rhodamine 6G	1 pM	(Zhang, Wang et al. 2019)
Microfluidic SERS chip based on Ag-Au nano composite and ITO as support platform	Deposition of the Ag-Au NC on ITO by electrodeposition and galvanic replacement	Melamine detection	0.1 nM	(Wang, Xu et al. 2017)

Table 2:

Material	Fabrication method	Application	LOD	References
Copper nanowires coated CF	Electrophoretic deposition	Sensing of designer drugs	10^{-10} – 10^{-12} M	(Halouzka, Halouzkova et al. 2017)
CF bearing ZnO nanosheet coated with Ag nanoparticles	A combination of Atomic layer deposition, pyrolysis and ion-sputtering	Methyl parathion (MP) and PCB-77	0.1 µM for MP and 5 µM for PCB-77	(Wang, Meng et al. 2014)
CF coated with Au nanoparticles	Electrochemical deposition	Paraoxon	10 mM	(Tran, Fallatah et al. 2018)
CF bearing ZnO nanorods that is coated with Ag nanoparticles	Hydrothermal growth of ZnO nanorods followed by electrostatic deposition of Ag^+ and chemical reduction Ag^+ ions to Ag nanoparticles	Phenol red	1 nM	(Huang, Xu et al. 2016)
CNT/AuNP hybrid	Chemical method	Melamine in milk	1 nM	(Zhang, Ji et al. 2015)
Ag nanoparticles on CF	Chemical deposition using an incubator shaker method	2,4 dinitrotoluene	50 ppm	(Mbah, Moorer et al. 2013)
Au nanoparticles on CF needles	Electrodeposition of Au nanoparticles on CF needles	Acetamiprid	0.05 µg/mL	(Kang, Wu et al. 2018)
MWCNT decorated with Ag nanoparticles	Thermal oxidation MWCNTs and surface functionalization with OH- and/or COOH followed by photochemical deposition of AgNPs	Methylene blue	1 ppm	(Dinh, Huy et al. 2016)

Table 3:

Material	Fabrication method	Application	LOD	References
Si wafer with Ag nanodendrites	Electroless deposition	For PCB77 detection	10^{-10} M	(Yang and Meng 2010)
Cu nanoparticles on Si wafer	Si–H bond assisted assembly of Cu NPs	Sudan-I dye	1 nM	(Shao, Que et al. 2012)
AgNPs bearing Si nanocones on Si wafer	Plasma etching and ion sputtering	Detection of dimethyl phthalate	10^{-7} M	(Zuo, Zhu et al. 2015)
Si wafer with Si nanopillars bearing AgNPs	Electroless deposition	Detection of melamine	10^{-5} M	(Liu, Wu et al. 2018)
Si wafer bearing Si nanowires (Si NW) that is coated with AgNP	Si NW synthesis by metal-assisted chemical etching followed by AgNP coating using dopamine	Detection of methyl blue	1 mM	(Akin, Yilmaz et al. 2014)
Au nanoparticles on a thiol bearing Si wafer	Thiolation of Si wafer surface and subsequent immersion into AuNPs	Detection of Ricin	47.5 ng /mL	(Tang, Sun et al. 2016)
Standing Au nanorods (AuNR) on Si wafer slide	Seed mediated synthesis of Au NR in CTAB and subsequent drop casting of Au NRs	Carbaryl detection	2.5 ppm	(Zhang, Yu et al. 2015)
Si wafer with Si nanowires (SiNW) decorated with AgNPs	SiNW synthesis by vapor–liquid–solid (VLS) process using a Sn catalyst followed by addition of $AgNO_3$ solution	Carbaryl detection	0.01 mg mL	(Han, Wang et al. 2012)
Au nanoparticles on a ZnO nanorods (ZnO NRs) bearing Si wafer	Hydrothermal preparation of ZnO NRs followed by sputtering of Au	Detection of Methyl blue	1 pM	(Sinha, Depero et al. 2011)
Q-SERS™ (Au nanostructures on Si wafer)	Commercial SERS substrate	Azinphos-methyl (AM), phosmet and Carbaryl	2.94 ppm for AM, 2.91 ppm for phosmet and 5.35 ppm for Carbaryl	(Liu, Zhou et al. 2013)

AgNPs on Si wafer that is coated with Cr and Au film	Si wafer coated sequentially with a layer of Cr and Au. This was followed by surface modification with APTES and subsequent conjugation with Ag NPs	Thiram detection	0.24ppm	(Guo, Xiao et al. 2015)
ZnO NRs decorated with AgNPs on Si wafer support platform	Electrochemical growth of ZnO NRs(after ZnO Seeding) followed by sputtering of AgNPs	Detection of PCB-77	3µM	(Tang, Meng et al. 2012)
Si wafer coated with calixarene functionalized Ag nanoparticles	Spin coating of Si wafer with thiolated calixarene in $AgNO_3$ solution followed by thermal reduction of $AgNO_3$	Detection of pyrene and naphthalene	3 x 10^{-10} mol/l for pyrene and 13 x 10^{-9} mol/l for naphthalene	(Kwon, Sowoidnich et al. 2012)
AgNPs on Si wafer	Surface modification of Si wafer using (3-aminopropyl) trimethoxysilane followed by its immersion into silver–ammonia solution for in situ growth of AgNPs	Rhodamine 6G	10 pM	(Tu, Li et al. 2018)
Si wafer bearing sunflower-like nanoarrays decorated with AgNPs	Preparation of sunflower-like nanoarrays by spin coating colloidal silica spheres onto Si wafer. This was followed by AgNP deposition via sputtering	Melamine	0.1 µM	(Zhang, Xiao et al. 2017)
Ag nanorods (AgNRs) arrays on Si wafer	Growth of AgNRs embedded in polydimethylsiloxane (PDMS) on Si wafer by glancing angle deposition method followed by removal of PDMS	Thiram	1 µM	(Kumar, Goel et al. 2017)

AgNP-decorated silicon wafer	Growth of AgNPs by hydrofluoric acid-assisted etching Method followed by 4-aminothiophenol attachment as an internal standard	Pb(II) and Hg(II) ions	19.8 ppt for Pb(II) and 168 ppt for Hg(II)	(Shi, Chen et al. 2018)